UNIVERSITY OF LEICESTER

SCHOOL OF ENGINEERING

(Control System Design and MPPT tracking of PV panels under different conditions)

Module code:	**EG7020**
Module name:	**MSc Individual Project**

Date of submission 27/Sep/ 2022

Author(s):	**Qusay Hatem Issa Alsultan**
Student ID(s):	**209013733**
Degree:	**Advanced electric and electronic MSc**
Tutor/Project supervisor:	**Dr Andrea Lecchini Visintini**

SUPERVISOR'S COPY/EXAMINER'S COPY [For 3rd/4th year projects only - delete as appropriate]

Summary

Recently, renewable energy sources have grown as the population to cover all their daily needs. One of these environmentally friendly sources is photovoltaic solar cells, whose I-V and P-V depend on the weather conditions. The challenge is making this source produce or work at the maximum power point (MPP). Although some previous studies have discussed this problem, some of their results have poverty in performance. Therefore, a new method is introduced in this project to track the MPP under two scenarios, one by fixing the temperature and irradiance changes, and the second one is the opposite. The proposed model is implemented using MATLAB Simulink. In addition, the DC-DC boost converter and (p&o) algorithm with two PI controllers are used to control the solar system. Before that, the system's controllability, observability, and stability are satisfied appropriately. The results show that the proposed system did very well. The chosen design's performance, speed, efficiency, and oscillation are significantly better when compared with the previous method mentioned in the literature. Although this project can be installed and applied in reality, partial shading is not considered because it needs a complex control design to achieve the desired goals.

ACKNOWLEDGMENTS

This project becomes a reality with many individuals' kinds of support and help. I want to extend my sincere thanks to all of them.

I am deeply indebted all my teachers at university of Leicester and especially to my supervisor Dr Andrea Lecchini Visintini. I appreciate all his time, ideas, and funding contributions to make my master's experience productive and stimulating. I am also thankful for the excellent personal tutor Dr Warrington Paula F.T, for her support. Also, thanks to the postgraduate student director Dr Hussain Zahir for his efforts and response to my questions. I express my heartful thanks to my country (Iraq) for giving me the chance to study in a country like the UK, and Iraqi Cultural Attaché, London, for their help.

I would like to thank my sponsor, the university of Anbar, for their support and help. I will not forget the staff of Anbar's renewable energy research centre for their support.

I dedicate my project to my parents, whose love, prayers, blessings, and inspiration enable me to come out with this work.

I should never forget the love, support and endless wishes from my wife, engineer Remah Alsultan and My lovely Kids. I owe sincere and earnest thankfulness to my dearest Brothers and sisters for their encouragement and support.

Finally, I offer my regards and blessings to all my relatives and friends who supported me in any respect while completing my master's study.

Contents

List of abbreviations

C	Converter filter capacitance	PI	proportional and integral controller
d	Converter duty cycle	L	Inductance of the converter
f	Switching frequency, Hz	P&O	Perturb and observe algorithm
I	Output current of solar cell, A	PWM	pulse width modulator
Impp	Output current of solar cell at maximum power point	T_{ref}	reference temperature
I_{rs}	Reverse saturation current	G_{ref}	reference irradiance
Io	Output current from converter, A	R_{sh}	shunt resistance
Is	Input current to converter, A	R_s	series resistance
G	Irradiance	E_g	threshold voltage
MPPT	maximum power point tracker	N	cells connected in parallel
PV	photovoltaic	n	cells connected in series
P-V	Power- voltage characteristics	k_p	proportional gain
I-V	Current- voltage characteristics	k_i	integral gain
D	Diode		

List of figures

List of tables

1 Introduction

Nowadays, there is a tendency to rely on renewable energy sources since they are environmentally friendly and have low maintenance costs, such as Solar energy, wind energy and hydrology power (Fuentes et al., 2020). A photovoltaic (PV) solar system is an electronic circuit that receives sunlight and converts it to electricity (Taha et al., 2011). The output power of the solar cell depends on certain conditions, such as sunlight intensity and temperature. Baimel et al., 2019 found that varying irradiance affects the PV voltage, while the current is more sensitive to temperature changes, which led to the fact that the relation between PV power and external conditions is nonlinear. Due to this nonlinearity, each panel has one maximum power point (MPP) under specific conditions (Anoop et al.,2018). At this point, the maximum power and efficiency can be achieved from the solar panel. In a country like the UK, the irradiance and the temperature change rapidly during a short time (Barrow et al., 1996). Therefore, making the solar panel works at the MPP can be considered a challenge.

1.1 literature studies

Recently, some studies have been done to track the maximum power point of solar cells. For instance, Kandgaonkar, R. et al.,2013 obtain a pulse width modulator (PWM) as a control input into a single-phase inverter to track the MPP. Esram, T. et al.,2007 discuss some control algorithms and compare them. Murtaza, AF et al. (2013) Compare (p&0), incremental inductance and fractional open voltage algorithms. Furthermore, Verma, D et al.,2022 introduced a new method by matching the impedance of the panel and the load using a DC-DC converter. However, these studies have complexity, high cost, and oscillation issues. In this paper, a new method will be used by using two PI (proportional and integral) controllers with the P&O MATLAB algorithm to control the duty cycle of a dc-dc boost converter.

1.2 The structure of the solar cell

The equivalent photovoltaic circuit can be represented in fig 1 (Taha et al., 2011). A diode is connected parallelly with a current source. Physically, the solar cell consists of two semiconductor layers. These layers absorb the radiation from the sun and transfer it as energy for its electrons. With this energy, the electrons inside the semiconductor flow from one layer to another, producing the electric current. The output power increases with the irradiance increase and decreases with the rising in the temperature. Practicality, one single solar cell produces approximately 2 watts. Therefore, a group of solar cells can be connected parallelly or serially to approach the required power. Different solar panel modules depend on their provider company. Each company has a standard specification written on the panel's datasheet.

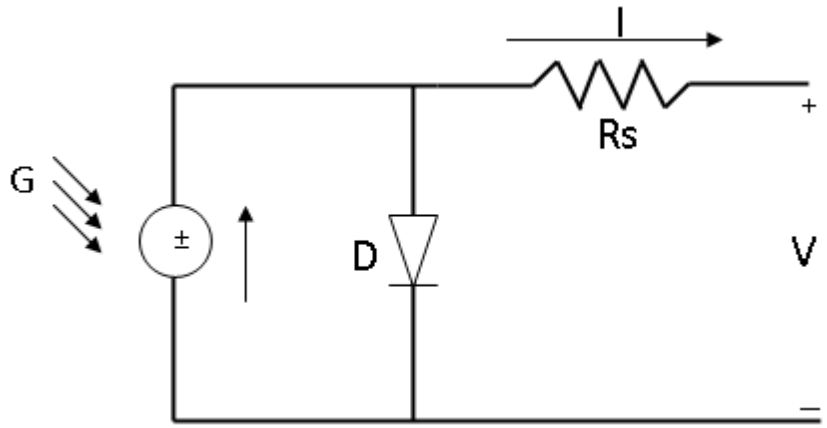

Figure 1.Solar cell circuit

1.3 Main problems

1.3.1 Tracking the maximum power of a solar panel system

Solar panel power, current, and voltage are affected by changes in external conditions (Irradiance and temperature). Hence, the problem is that the MPP will change with the input parameters change. MPP can be achieved when the load's impedance is equal to the impedance of the solar panel system (Nguyen et al., 2020). However, matching the load and the internal impedances of the PV array is impossible. Because of that, the control algorithms are causal to increase efficiency.

1.3.2 Tuning the PI controller

Conclusively the work at the MPP, a proportional and integral controller can control the boost converter's duty cycle. However, choosing the values of the PI gains (Kp, Ki) is difficult. The appropriate tuning of one PI controller performs well for tracking the maximum power point (Anto E et al., 2016). However, tuning one PI controller only works when the Irradiance is more than 500 W/m2. In other words, the maximum efficiency cannot be produced when the sun intensity falls beyond the threshold value. Therefore, two PI controllers could be tuned to solve this problem and ensure that the solar panel array produces maximum power under different disturbances.

2 Method

2.1 PV solar model

As mentioned above, the solar cell circuit can be formed as a photocurrent source parallel to one diode. Fig 2 shows the equivalent circuit of the photovoltaic cell after adding the series and parallel resentences (Abd El-Basit, 2013).

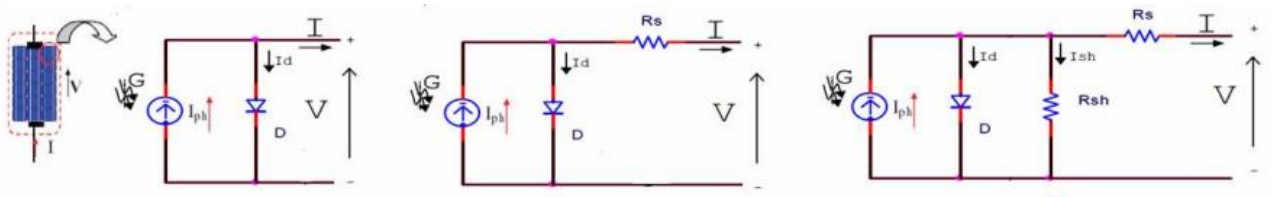

Figure 2.the equivalent circuit after adding the series and parallel resentences

Applying Kirchhoff's current law for the circuit shown above, the output current can be written as the equation below.

$$I = I_{ph} - I_s\left[\exp\left(\frac{V + IR_s}{nV_T}\right) - 1\right] \qquad (1)$$

Where I = output current, I_s = saturation current, V= output voltage, R_s = series resistance, n = quality factor of silicon about 1.1, V_T= thermal voltage which equal to

$$V_T = \frac{KT_c}{q} \qquad (2)$$

K= Boltzmann's constant 1.38 · 10−23 J/K

T_c= whether temperature

q= charge of the electron $1.6 * 10^{-10}$ c

Equation (1) does not accurately depict the solar panel's performance under changing environmental conditions. For this reason, R_{sh} is used with R_s for more practical accuracy. As shown in Fig 2, an extremely high value of R_{sh} is in parallel with the diode, while R_s is minimal (Kashif I et al., 2011). The current equation after adding becomes as shown below (Rikesh S et al.,2013).

$$I = I_{ph} - NI_s\left[\exp\left(\frac{V + IR_s}{nV_T}\right) - 1\right] - \left[\left(\frac{V + IR_s}{R_{sh}}\right)\right] \qquad (3)$$

The photocurrent (I_{ph}) is more sensitive to the change in sunlight intensity and the working temperature of the photovoltaic cell, as shown in the equation below (Pandiarajan N et al., 2011, Rikesh S et al.,2013).

$$I_{ph} = \left[I_{sc} + K_1(T_c - T_{ref})\right]\frac{G}{G_{ref}} \qquad (4)$$

Where I_{sc} = short circuit current of the panel; K_1= temperature constant at short circuit current, T_{ref}= the standard temperature of the solar cell; G = irradiance from the sun in W/m^2, G_{ref}= reference sunlight intensity in W/m^2. On the other hand, the saturation current in equation (3) is affected by the temperature change, as described below.

$$I_s = I_{rs}\left(\frac{T_c}{T_{ref}}\right)^3 exp\left[\frac{qE_g}{nk}\left(\frac{1}{T_{ref}} - \frac{1}{T_c}\right)\right] \qquad (5)$$

Where E_g = threshold voltage for the silicon 1.1 V, I_{rs} = dark reverse saturation current, and it can be derived below, Vo is the open circuit voltage (zero output current).

$$I_{rs} = \frac{I_{sc}}{exp\left(\frac{V_o q}{nkT_c}\right) - 1} \qquad (6)$$

The power-voltage and current-voltage characteristics of the solar panel can be found by implementing the equations mentioned above in MATLAB Simulink. Figures 3 to 5 show the block diagram of each equation.

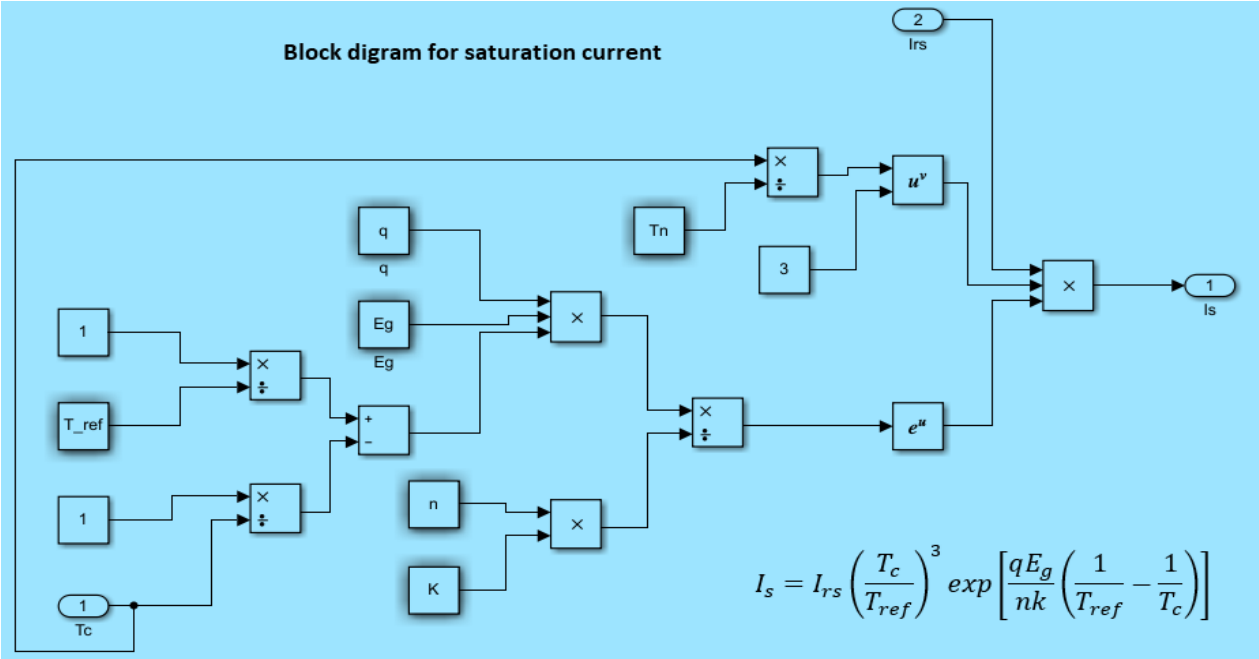

Figure 3.block diagram of Saturation current

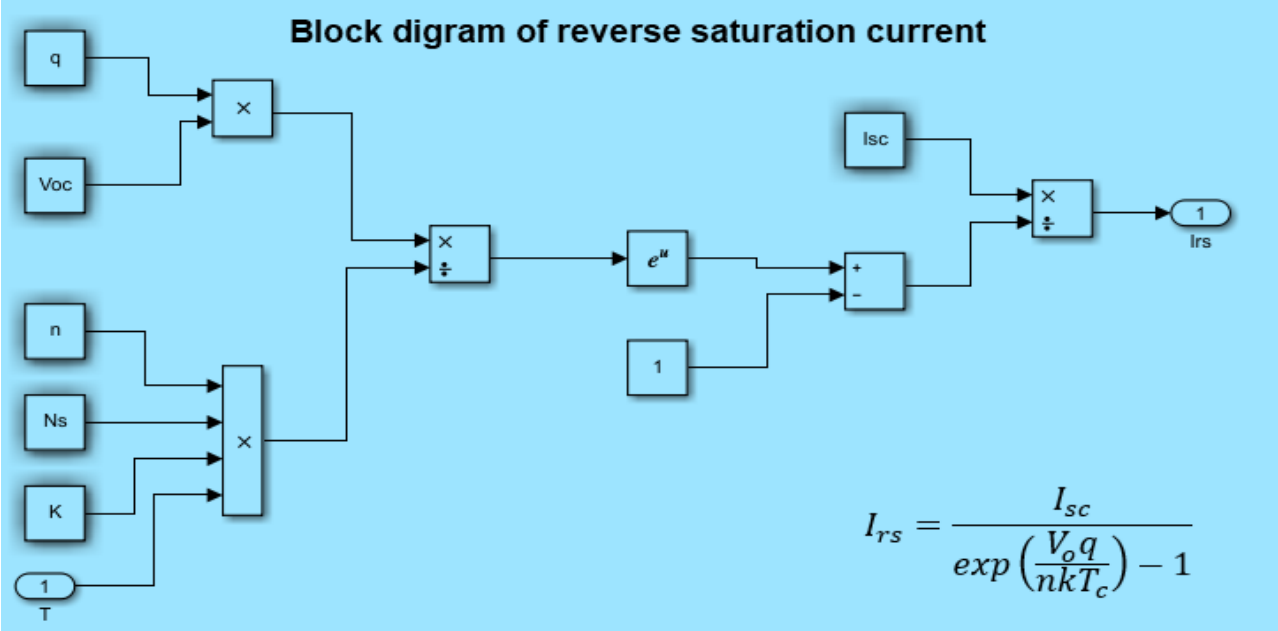

Figure 4.block diagram of reverse saturation current

Setting the values of reference irradiance (G_{ref}) to 1000 W/$m^2$and the reference temperature(T_{ref}) to (273 + 25 c), these two parameters are considered standard solar cell conditions. On the other hand, G and T_c are chosen as variables to show their effect on the maximum power point of the photovoltaic.

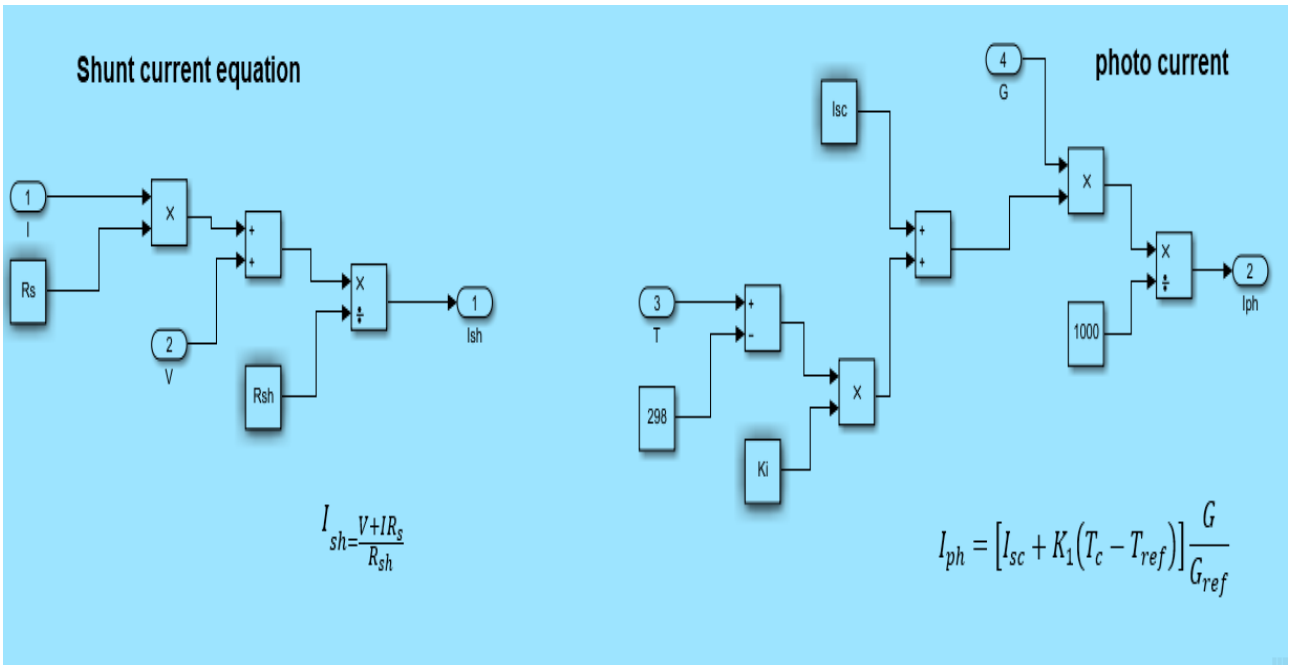

Figure 5.shunt current and photocurrent block diagrams

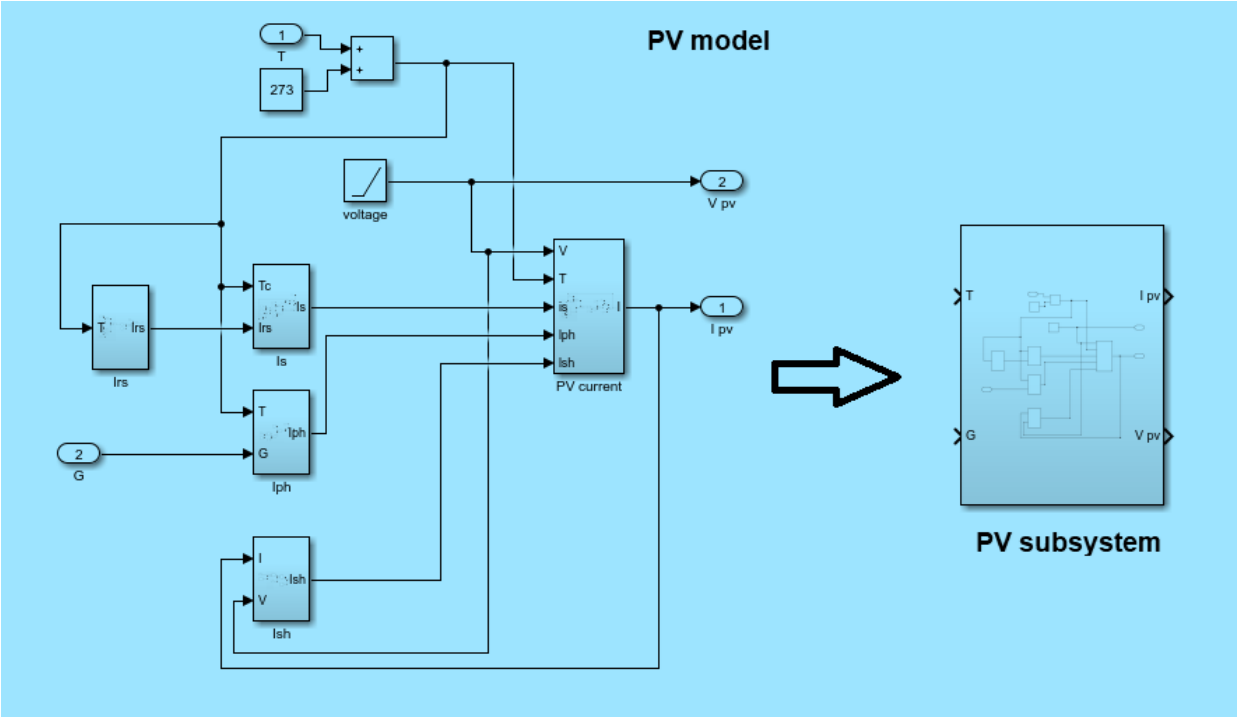

Figure 6.Photovoltaic mathematical model

After completing the mathematical model of the solar cell, it comes to choosing the solar panel module and its rated power. For this framework, the 1soltech 1sth-215-p solar panel module has been chosen. Practically, the rated desired power under slandered conditions (G= 1000 W/m^2, Temp= 25 c) is 100 KW. Table (1) shows all the parameters set in the Simulink variables to produce the desired power (Solar Hub - PV Module Details: 1STH-215-P - by 1Soltech, 2022).

Table 1.the parameters of the PV system

Power at STC (W)	215
Power at PTC (W)	189.4
Bifacial	No
N	47
n	10
Power Density at STC (W / m^2)	136.943
Power Density at PTC (W / m^2)	120.637
Vmp: Voltage at Max Power (V)	29.0
Imp: Current at Max Power (A)	7.35
Voc: Open Circuit Voltage (V)	36.3
Isc: Short Circuit Current (A)	7.84
Nominal Operating Cell Temp (°C)	47.4
Open Circuit Voltage Temp Coefficient (% / °C)	-0.361
Short Circuit Current Temp Coefficient (% / °C)	0.102
Max Power Temp Coefficient (% / °C)	-0.495

2.1.1 The effect of Irradiance (constant temperature 25 c)

The most significant parameter affecting the solar cells' performance is the irradiance (G). it is the light intensity that comes from the sun. It is measured in Watt/m2. As mentioned above, PV current is more affected by the change in irradiance. From equation (4), when G increases, the PV current increase while it decrees by minimizing the radiation. This varying solar panel current will change the position of the maximum power point. Because of this change, the control system is casual. Fig (7) shows the P-V and I-V characteristics of the solar cell with different irradiances and constant temperatures.

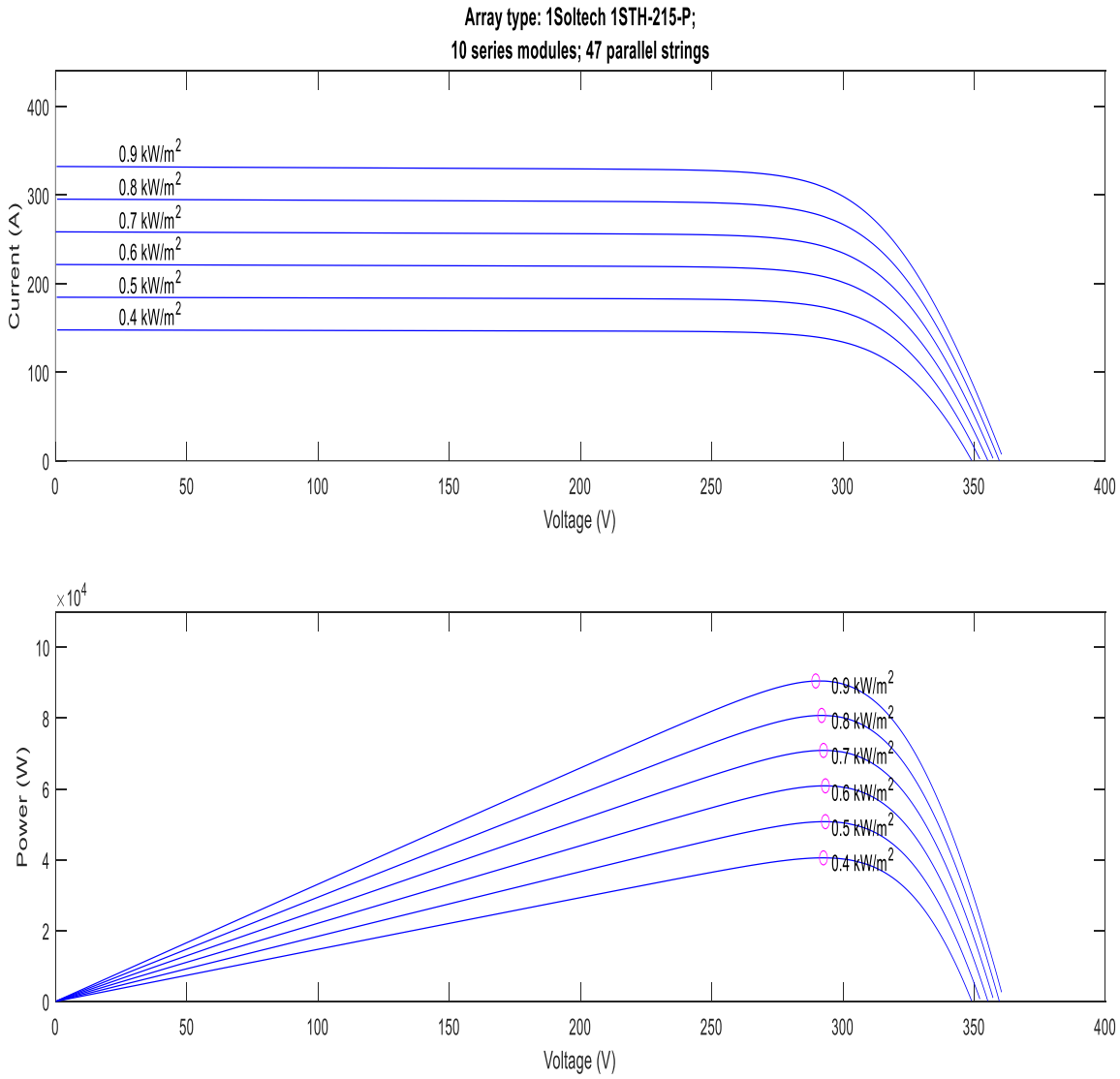

Figure 7.P-V and I-V characteristics under different radiations (constant temperature)

2.1.2 The effect of temperature (constant irradiance 1000 W/m^2)

In addition to the sunlight intensity, the temperature can play an essential role in the behaviour of the maximum power point of the photovoltaic system. For instance, in figure (8), PV voltage is more sensitive to temperature changes. In contrast to the irradiance, the temperature has inverse proportional to the power and voltage. Its raising produces less performance and efficiency. The reason is that the saturation current is temperature depends, and that is clear from equation (5) that Is has cubic direct proportional with the temperature. Increasing in Is leads to minimizing the PV current and the solar power, as shown in equation (3).

The instability of the two mentioned conditions led to a change in the position of the maximum working point. Tracking this point and maximizing the efficiency need the efforts of the MPPT control algorithms. These techniques control the voltage by moving it to the MPP throw the DC-DC boost converter.

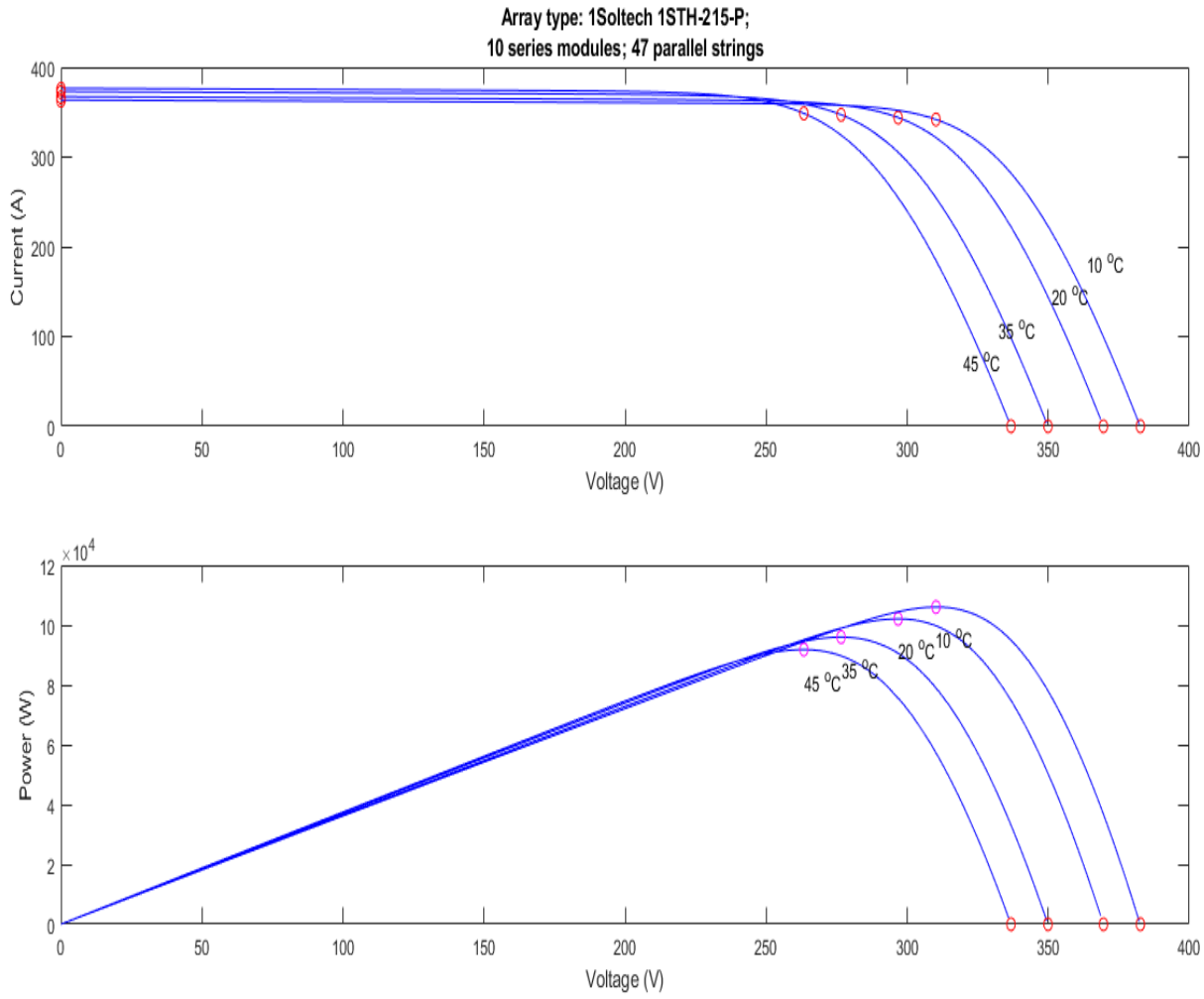

Figure 8.P-V and I-V characteristics under different temperatures (constant irradiance)

2.2 Modelling the MPPT circuit

The PV system must be built with a maximum power point tracking (MPPT) circuit integrated between the PV module and load to operate at MPP in response to variations in the external conditions. This circuit contains two internal systems. the first is a DC-DC converter, and another is a control circuit.

2.2.1 DC-DC Boost converter

A DC converter can be used to transfer the maximum power from the solar panel to the load. There are plenty of kinds of converters that can do the same work, such as boost, buck, and buck-boost. For this project, the boost converter has been selected and designed. Converting the variable input voltage to a higher stable output value is the boost converter's function, which comprises the switch Q, the inductor L, the output diode D, and the output capacitor C_0. The high efficiency of DC-DC converters is ideally due to the shallow power consumption of all these devices (Nguyen et al., 2020). the MOSFET is chosen as a switch, and the PI controller easily controls its gate by the duty cycle, which can take two states on and off. T is the period for one duty cycle. In the inductor (L), The energy will be stored during T-ON. However, when the gate is open, the inductor polarity will be reversed and added with PV voltage to maximize the voltage at the load via the diode (D). Figure (9) shows the simple design for the boost converter with its components. Ci and Co are installed to reduce the oscillations in the input and output voltages.

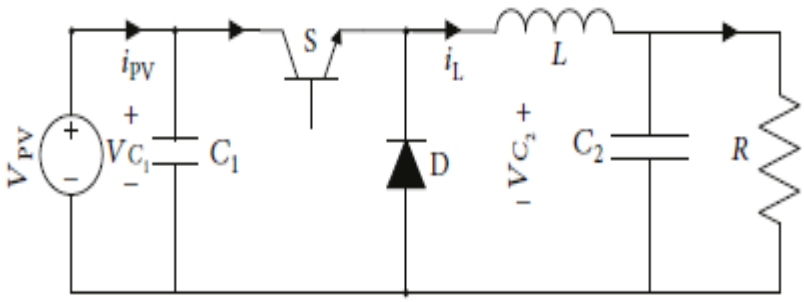

Figure 9.DC-DC Boost converter circuit

2.2.1.1 State space representation of the DC converter

The working principle of the boost converter is based on two complementary operation modes, namely CLOSED (T-on) and OPEN (T-off) modes. As mentioned above, in closed mode, the inductor stores energy. While in open mode, the capacitor Ci releases the energy to the output. Under ideal conditions, two fundamental principles are behind the boost converter's behaviour: The energy-balanced principle (volt-second balance) and the charge-balanced principle (Gandomkar et al., 2016).

From the first principle, the input energy is equal to the output energy:

$$P_{in} = P_{out} \longrightarrow I_{in}V_{in} = I_{out}V_{out} \qquad (2.1)$$

second principle implies the input charge equal to the output charge;

$$Q_{in} = Q_{out} \longrightarrow I_{in}(1-d)T = I_{out}T \qquad (2.2)$$

Based on these two principles, the relation between the output and input voltages of the boost converter given by;

$$V_{out} = \frac{V_{in}}{1-d} \qquad (2.3)$$

Where d is the duty cycle, its value is between 1 and 0, meaning that V_{out} is always greater than V_{in}(Nelson, 2011). The DC-DC boost converter is modelled by applying the averaging method for both modes (Mahdavi et al., 1997).

$$\dot{x} = A_1x + B_1u \quad \text{(switch closed mode).} \qquad (2.4)$$

$$\dot{x} = A_2x + B_2u \quad \text{(switch open mode).} \qquad (2.5)$$

Then the average state model is:

$$\dot{x} = \bar{A}x + \bar{B}u \qquad (2.6)$$

Where:

$$\bar{A} = A_1d + A_2(1-d) \qquad \bar{B} = B_1d + B_2(1-d)$$

During the closed mode (T-on) the circuit diagram is shown as below. Noting that Ci has been cancelled from the circuit for simplicity.

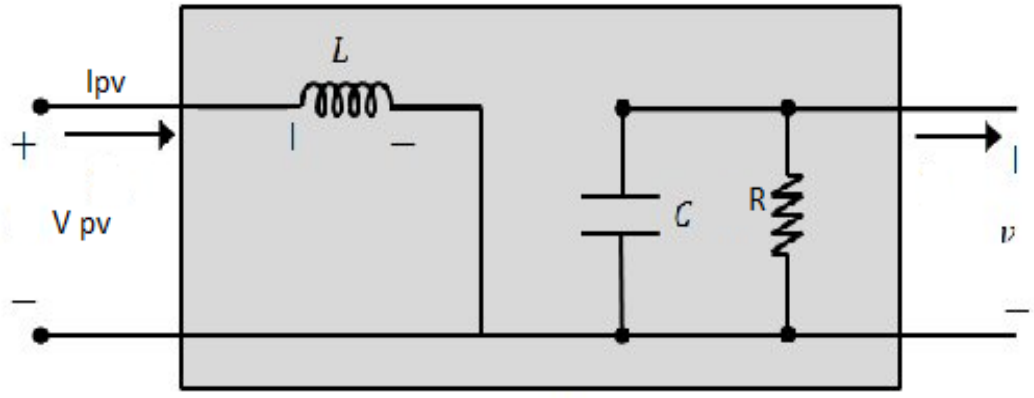

Figure 10.DC-DC Boost converter circuit during close state

From figure (10) (Mayo, J et al., 2021), the resulting dynamic state equations given by:

$$L\frac{di_L}{dt} = V_{in} \qquad (2.7)$$

$$C\frac{dv_c}{dt} = -\frac{V_c}{R} \qquad (2.8)$$

Note that:

$i_L = i_{in}$= the current of the inductor

$v_c = v_{out}$= the voltage of the capacitor

Let state the variables:

$x_1 = i_L \ ; x_2 = v_c$

And the output equation;

$y = v_c = x_2$

There for the state space equations for the closed mode can be written as;

$$\begin{vmatrix}\dot{x}_1\\ \dot{x}_2\end{vmatrix} = \begin{vmatrix}0 & 0\\ 0 & -1/RC\end{vmatrix}\begin{vmatrix}x_1\\ x_2\end{vmatrix} + \begin{vmatrix}1/L\\ 0\end{vmatrix}V_{in} \qquad (2.9)$$

$$\dot{x} = A_1 x + B_1 u$$

Now, when the switch is open, the equivalent circuit of the boost converter shown is shown below (Mayo, J et al., 2021).

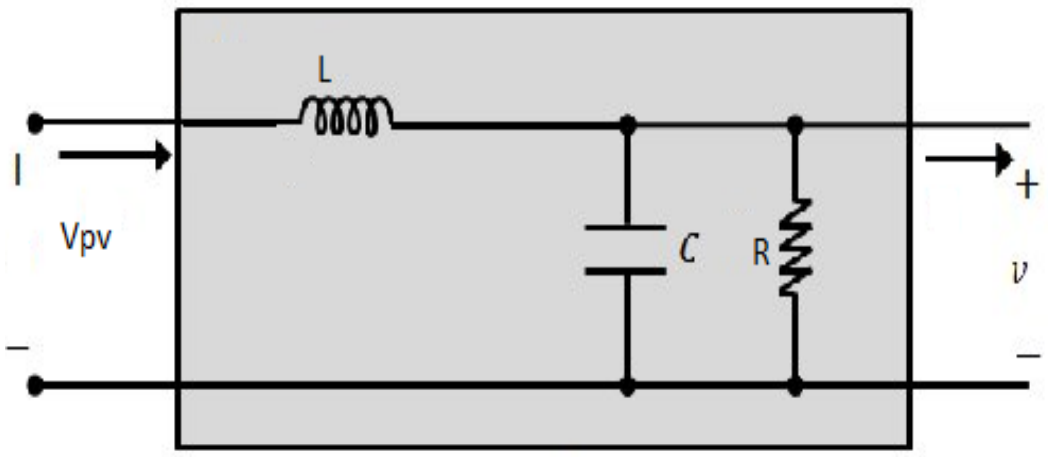

Figure 11.DC-DC Boost converter circuit during open state

From figure (11), the dynamic state equations can be given as:

$$L\frac{di_L}{dt} = V_{in} - V_c \qquad (2.10)$$

$$C\frac{dv_c}{dt} = i_L - \frac{V_c}{R} \qquad (2.11)$$

then, the state space equations for the open mode can be written as;

$$\begin{vmatrix}\dot{x}_1\\ \dot{x}_2\end{vmatrix} = \begin{vmatrix}0 & -1/L\\ 1/c & -1/RC\end{vmatrix}\begin{vmatrix}x_1\\ x_2\end{vmatrix} + \begin{vmatrix}1/L\\ 0\end{vmatrix} V_{in} \qquad (2.12)$$

$$\dot{x} = A_2 x + B_2 u$$

The averaging method (equation 2.6) combines the linearized state space equations for both modes to obtain the following:

$$\begin{vmatrix}\dot{x}_1\\ \dot{x}_2\end{vmatrix} = \begin{vmatrix}0 & \frac{-(1-d)}{L}\\ \frac{1-d}{C} & -1/RC\end{vmatrix}\begin{vmatrix}x_1\\ x_2\end{vmatrix} + \begin{vmatrix}1/L\\ 0\end{vmatrix} V_{in} \qquad (2.13)$$

And the output equation is:

$$y = |0 \quad 1|\begin{vmatrix}x_1\\ x_2\end{vmatrix} + 0 \qquad (2.14)$$

In this proposed framework, table (2) shows the specifications required to design the boost converter. These specifications should match the parameters of the solar panel, which are mentioned in table (1), to achieve the desired power.

Table 2.proposed specifications of the DC-DC boost converter

Input voltage = $\boldsymbol{V_{in}}$	250 – 350 V
Output voltage = $\boldsymbol{V_o}$	500 V
Output current = $\boldsymbol{Io}$= rated power/output voltage	200 Amp
Rated power	100 Kw
Switching frequency	5 KHz
Voltage ripple $\boldsymbol{\Delta v_o}$	1%
Current ripple $\boldsymbol{\Delta i}$	29.0

From table (2), the values of the converter's inductor and capacitor can be calculated using the following formulas (Salman et al., 2018).

$$L = \frac{v_i(v_0 - v_i)}{\Delta i \, f_s v_o} = 1.25\, mH$$

$$C = \frac{i_o(v_0 - v_i)}{\Delta v_o \, f_s v_o} = 4000\ \mu f$$

After finishing the modelling of the plant, it comes to designing an appropriate control circuit to make the plant always track the maximum power point. Before that, it will be interesting if the plant's controllability, observability, and stability are tested.

2.2.2 Control circuit design

In a control system, there are three essential basic concepts that the designers should follow. checking the controllability of the plant, testing the observability, and finally, proving the system's stability.

2.2.2.1 Controllability of the plant

The controllability of any system means the ability of the external force to drive the system's states from their initial values to the final states at a particular time. A system is considered accessible for "LTI (linear time-invariant) systems if and only if its controllability matrix has a full row rank of p, where p is the dimension of matrix A, and p*q is the dimension of matrix B" (Chen et al.,2006). Any state x1 that can be moved to the zero-state x = 0 in a limited number of steps is controllable, also known as "Controllable to the origin," in a system. In other words, when the rank of the controllability matrix equals the rank of the system matrix A, the system is controllable. Furthermore, another condition can be checked; if the determinant of the controllability matrix does not equal zero, it could say the plant is controllable. The general controllability matrix can be written as follows;

Ç= $[B \quad AB \quad A^2B \ldots A^{p-1}B] \in R^{p_x pq}$

From the state space equations of the boost converter, which are described above, matrixes A and B can be shown as;

A= $\begin{vmatrix} 0 & \frac{-(1-d)}{L} \\ \frac{1-d}{C} & -1/RC \end{vmatrix}$ B= $\begin{vmatrix} 1/L \\ 0 \end{vmatrix}$

From the general definition of the controllability matrix, it can be calculated for the proposed DC-DC converter as:

$$Ç = \begin{vmatrix} \frac{1}{L} & 0 \\ 0 & \frac{-(d-1)}{LC} \end{vmatrix}$$

And the determinate of the construability matrix can be found by using MATLAB command (det (Ç)) as;

$$\det(Ç) = \frac{-(d-1)}{L^2 C}$$

Substituting L and C with their values which are mentioned in table (2). The determinate of the controllability matrix does not equal zero. In addition, this matrix has a full rank equal to 2, which means the system is controllable.

2.2.2.2 Observability of the plant

Another significant check that the designers should follow before designing the control system is proving system observability. The plant's initial states x (0) can be determined from the output equation. In other words, the system is observable if the observability matrix (Q) has a full rank. This matrix depends on the plant's state matrix (A) and output matrix (C). The general definition of the observability matrix is shown as follows;

$$Q = \begin{vmatrix} C \\ CA \\ CA^2 \\ . \\ . \\ . \\ CA^{P-1} \end{vmatrix}$$

And matrixes A and C of the DC-DC boost converter are shown as below:

$$A = \begin{vmatrix} 0 & \frac{-(1-d)}{L} \\ \frac{1-d}{C} & -1/RC \end{vmatrix} \qquad C = |0 \quad 1|$$

Substituting A and B in the observability matrix Q to get the following

$$Q=\begin{vmatrix} 0 & 1 \\ \frac{1-d}{C} & -1/Rc \end{vmatrix}$$

This matrix has a full rank of 2, proving that the DC-DC boost converter is observable. After proving that the system is controllable and observable, checking the stability of the plant is required.

2.2.2.3 Stability of the plant

Any stable dynamic system is appropriately controlled and operates effectively under various operating situations. Stability is a desirable attribute of dynamic systems. Although there are many ways to check systems' stability, this paper has discussed the Bounded-Input Bounded-Output Stability (BIBO), internal stability, and Lyapunov criteria. to analyse the stability of the plant. For this reason, the transfer function of the DC-DC boost converter is required. It can be obtained from the state space matrixes by applying the Laplace transformation, as shown below;

The general state space equations of any system given as:

$$\dot{x} = Ax + Bu$$

$$y = Cx + Du$$

taking the Laplace transformation for each equation, assuming zero initial condition;

$$sX(s) = AX(s) + BU(s) \qquad (2.15)$$

$$Y(s) = CX(s) + DU(s) \qquad (2.16)$$

Simplify the input equation by putting X(s) in one side and U(s) in the other;

$$sX(s) + AX(s) = BU(s) \qquad (2.17)$$

$$(sI + A)X(s) = BU(s) \qquad (2.18)$$

Where I is identity matrix, so X(s) will become as;

$$X(s) = (sI + A)^{-1}BU(s) \qquad (2.19)$$

Substituting X(s) in the output equation, and assuming D = 0;

$$Y(s) = C(sI + A)^{-1}BU(s) + 0 \qquad (2.20)$$

Then, the transfer function $Y(s)/U(s)$ becomes as:

$$\frac{Y(s)}{U(s)} = C(sI + A)^{-1}B \qquad (2.21)$$

From this equation, the transfer function of the proposed DC-DC converter can be obtained by replacing the A, B, and C matrixes with the modelled ones mentioned above (equations 2.13 and 2.14). Noting that the values of L, R, and c are substituted from table 2, and d any value between 0 and 1.

$$G_{(s)} = \frac{12000}{S^2 + 125\,S + 72000} \qquad (2.22)$$

The step response of this transfer function can be shown in figure 12; it is clear that the plant has bounded input, and the output does not go to infinity. That means the plant is BIBO stable. The plant's response can be analysed using MATLAB command stepinfo(G(s)) since the rise time, maximum overshoot, and settling time can be calculated.

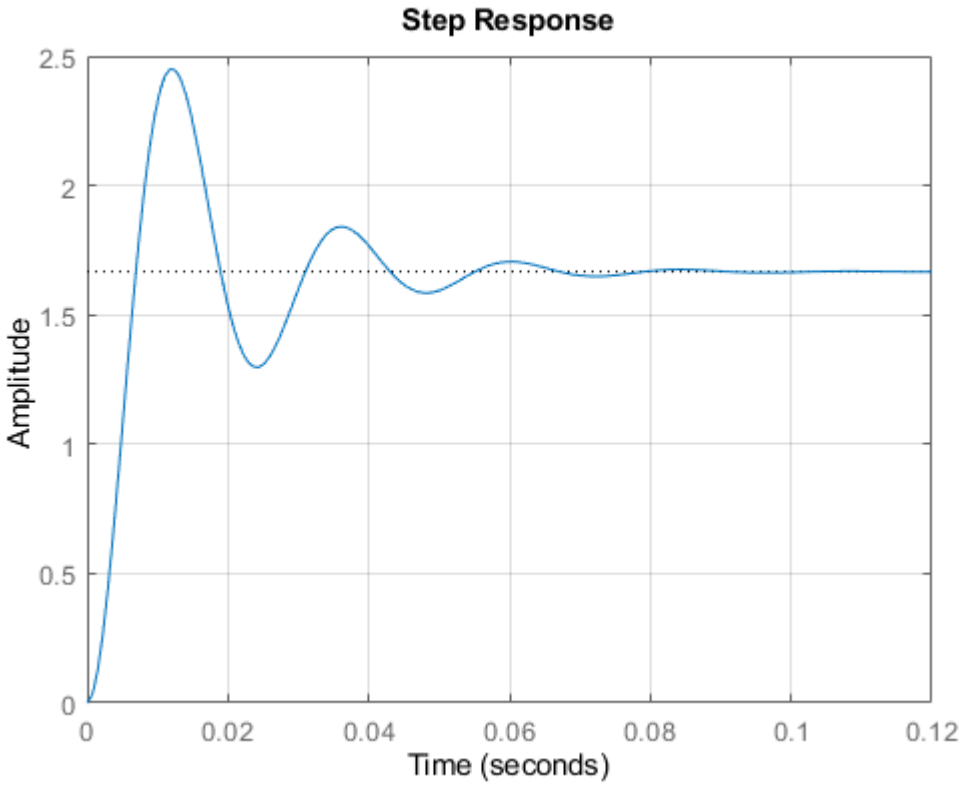

Figure 12.Step response of the DC-DC Boost converter

Regarding internal stability, figure 13 shows that the poles of the boost converter transfer function lie on the left-hand side (negative real roots). These poles can also be found by determining the eigenvalues of the A matrix. Pole (G) and eig(A) are two MATLAB commands that can determine the poles of any plant from its transfer function and state space representation.

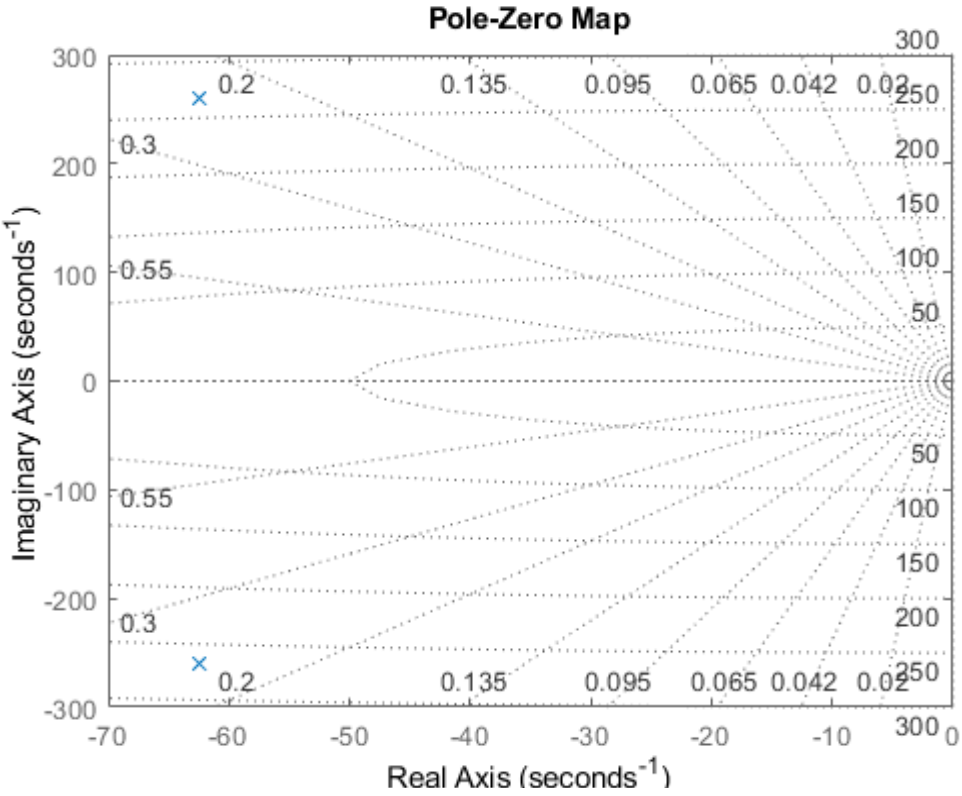

Figure 13.poles location

In terms of asymptotic stability, the Lyapunov technique can be checked. A *positive definite function* can be defined as an energy function; the system is considered asymptotic stable if the derivation of this energy function converges to or is less than zero (Li et al., 2021). Sabzi et al. (2016, p. 3) state some conditions related to the Lyapunov stability, which are described as follows;

$$\begin{cases} V(0) = 0 \\ V\cdot(x) < -\|x\| \\ lim\, V \to \infty; \|x\| \to \infty \end{cases}$$

Where V is the energy Lyapunov function, and x is the state variable.

In this frame work, lets choose an energy function equal to;

$$V = \frac{1}{2}x_2^2 \qquad (2.23)$$

The derivation of this function given as;

$$\dot{V} = x_2\dot{x_2} \qquad (2.24)$$

Substituting $\dot{x_2}$ from equation 2.13, equation 2.24 will become as;

$$\dot{V} = -\frac{1}{RC}x_2^2 + \frac{[1-d]}{c}x_1x_2 \qquad (2.25)$$

Equation 2.25 shows that the first term is always negative while the second term is unknown, and this can be solved by defining a new energy function, as shown below.

$$V = \frac{1}{2}x_2^2 + \Upsilon\, x_1^2 \qquad (2.26)$$

Where Υ is a positive definite constant, the new $\dot{V}$ will become;

$$\dot{V} = -\frac{1}{RC}x_2^2 + \frac{[1-d]}{c}x_1x_2 + 2\Upsilon x_1\dot{x_1} \qquad (2.27)$$

Substituting $\dot{x_1}$ from equation 2.13 and assuming the system is unforced (zero input), equation 2.27 will become as follows.

$$\dot{V} = -\frac{1}{RC}x_2^2 + \frac{[1-d]}{c}x_1x_2 - 2\Upsilon\frac{[1-d]}{L}x_1x_2 \qquad (2.28)$$

Setting the value of x equal to $\frac{L}{2C}$ will cancel the two unknown terms in equation 2.28. The only remaining term is $-\frac{1}{RC}x_2^2$. This term is always less than zero, and according to the conditions of the Lyapunov stability mentioned above, the system is asymptotic stable.

After proving that the proposed system is controllable, observable, and stable, the next step is formulating a MATLAB algorithm to decide the reference voltage of the maximum power point. This algorithm's error signal controls the stabiliser's duty cycle through two PI controllers.

2.2.2.3 Perturbation and observation algorithm

In order to reach the MPP of the PV array, many MATLAB algorithms can be used, such as incremental voltage and perturbation-observation algorithms. In this paper, the p&o algorithm has been introduced due to its simplicity. The PV module's power is varied by applying a slight disturbance in this method. Each time a measurement is made, the PV output power is compared to the old measured power. Two sensors have been used to measure the solar panel's voltage and current, which are entered into the MATLAB algorithm. The code of the proposed algorithm will be discussed later. Typically, for these two inputs, the instantaneous power of the solar cells can be calculated and saved in a specific memory. This process will be repeated periodically until the derivation of the power to time equals zero. Initially, a random starting voltage point was chosen as a reference.

Furthermore, the step size of the incremental or diminishing voltage has been chosen to equal two volts. This voltage could be added or subtracted to the reference one at a time (k). At the exact moment, the power is calculated and compared with the previous one, calculated at a time (k-1). If the added voltage increases the power, that means the chosen point lies on the left-hand side of the MPP; therefore, this increasing process keeps moving the point to the right until it catches the desired voltage (Dabra et al., 2017). Conversely, when the power decreases as the voltage is subtracted, the operating point lies on the right-hand side; hence more perturbations are needed to move the initial voltage to the left. This movement is controlled by the duty cycle of the DC-DC boost converter. It is increased if the new measured power is greater than the old one; however, the duty cycle will be decreased if the delta power is negative (Kumari et al., 2012) (Sera, Teodorescu, Hantschel and Knoll, 2008).

Figure 14 describes a brief explanation of the logical operation of the perturbation-observe algorithm (Hussein Selman, 2016). It depends on the selected starting operating point in which region to either increase or decreases the voltage.

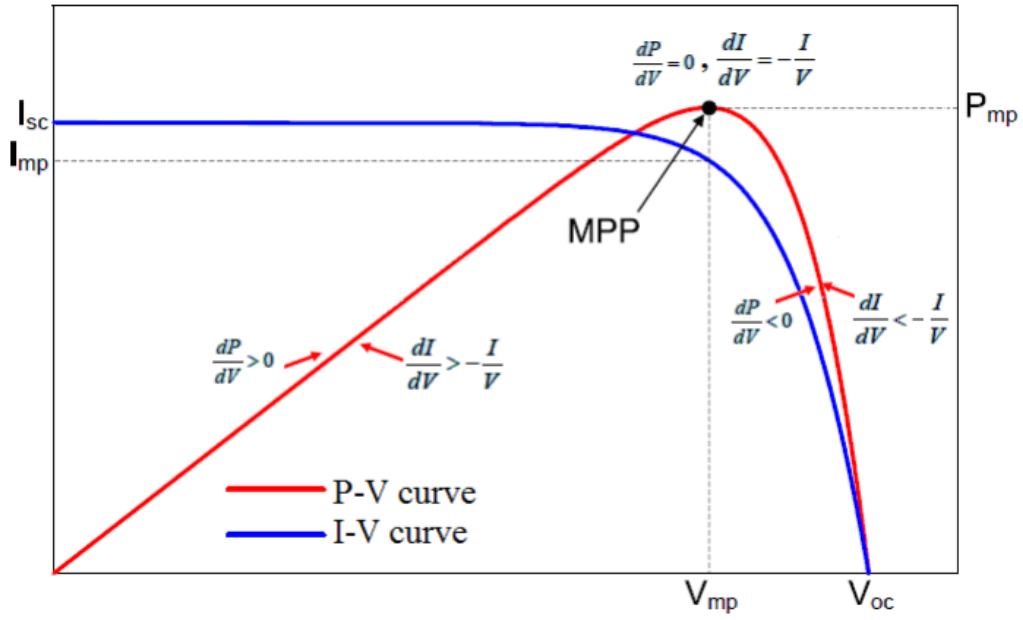

Figure 14. P&O Algorithm

For the most straightforward understanding, the below flow chart explains all the logical steps of the (P&O) algorithm (Salman et al., 2018). The process starts from the chosen starting point until achieving the maximum power point. In this algorithm, the biggest challenge is how the starting working point is chosen. The simplest way to sort that is by looking for the data sheet of the solar panel and making sure that the starting point is chosen below the open circuit voltage.

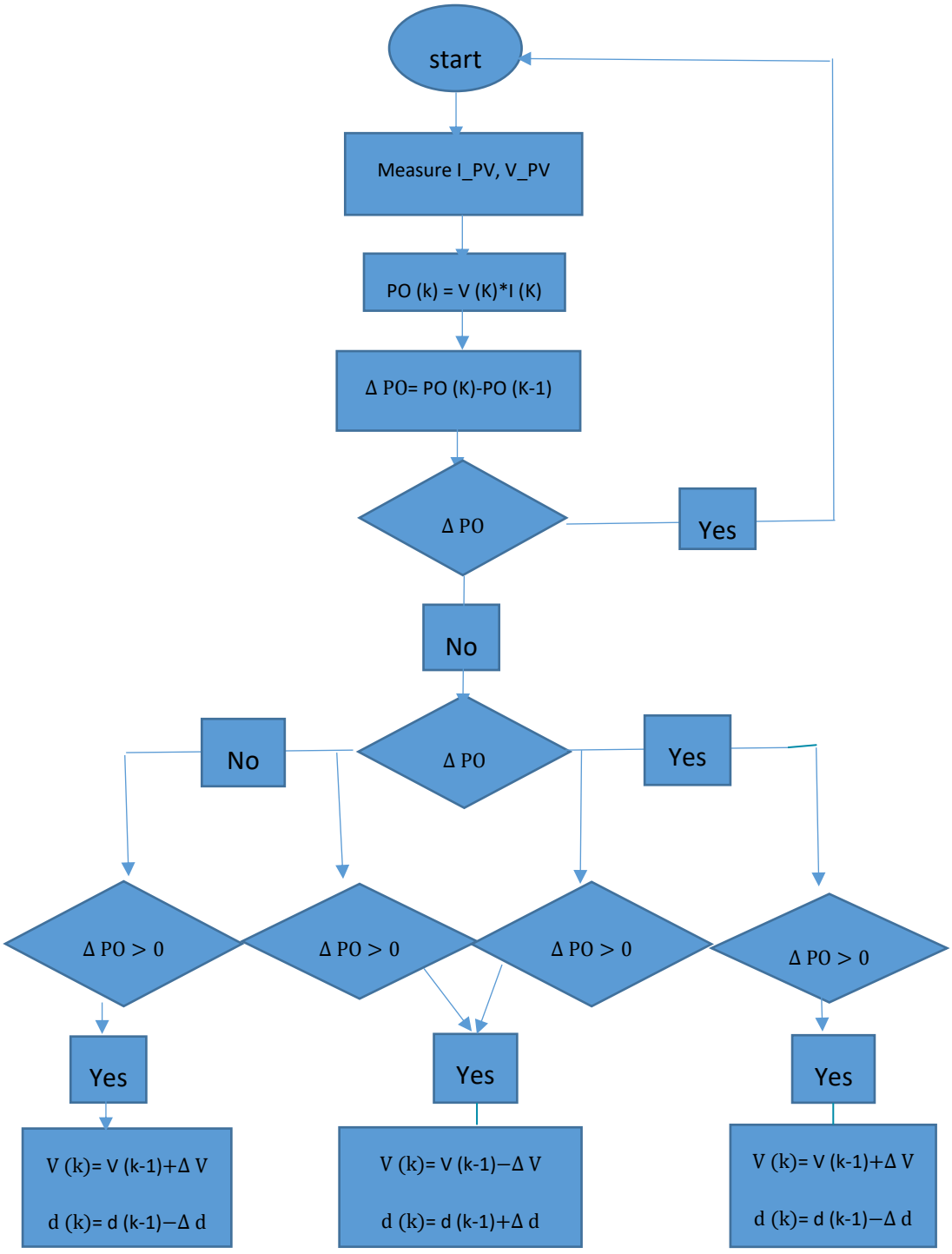

Figure 15.the flow chart of the perturb and observe algorithm

The proposed algorithm's logical steps, represented in the above flow chart, can be executed by the Simulink MATLAB function. The code is given below; it takes the inputs (PV voltage and PV current). This algorithm's output is the error, and the goal is to converge it to zero using PI control. So, the last step is designing a proportional and integral controller, in other words, finding the appropriate tunes for the gains of the proposed controller.

```
function RefV = Ref_Gen(V,I)

refrence_voltage_max=363; %the open circuit voltage from the datasheet of the solar panel
Refrence_voltage_min=0;        % the short circuit voltage always equal zero.
Refrence_voltage_intial=200; % starting point (should be less than open circuit voltage).
Delta_vrefernce=2;
persistent Old_voltage Old_power Old_refvoltage;
dataType='double';
if isempty(Old_voltage)
Old_voltage=0;            % defining a buffer to save the previous sample.
Old_power=0;
Old_refvoltage= Refrence_voltage_intial;
end
P=V*I;
delta_V=V-Old_voltage;
delta_P=P-Old_power;
if delta_P ~=0
    if delta_P<0
        if delta_V<0
            Ref_V= Old_refvoltage + Delta_vrefernce;
        else
          Ref_V= Old_refvoltage-Delta_vrefernce;
        end
    else
        if delta_V<0
            Ref_V= Old_refvoltage-Delta_vrefernce;
        else
            Ref_V= Old_refvoltage + Delta_vrefernce;
        end
    end
else Ref_V= Old_refvoltage;
end
if Ref_V>= refrence_voltage_max | Ref_V<=Refrence_voltage_min
    Ref_V=Old_refvoltage;
End

Old_refvoltage=Ref_V;
Old_voltage=V;
Old_power=P;
```

2.2.2.4 PI Controller and the tuning technique

The duty cycle of the DC-DC boost converter can be controlled by different techniques, such as the PID controller and pulse width modulator. Depending on the error from the P&O algorithm, one of these control methods can decide the suitable duty cycle to make the error as minimum as possible. Because of the worse performance of these methods and low efficiency, in this project, two PI controllers have been connected parallelly throw a selector switch. As mentioned above, the main problem of tuning one PI controller is insufficient when the irradiance falls below 500 W/m^2. Therefore, the selector has been chosen to activate one PI controller when the irradiance is between 1000 and 500 W/m^2. Otherwise, when it is less than 500, the second PI controller will be activated. Figure 16 shows the proposed control circuit taken from the Simulink.

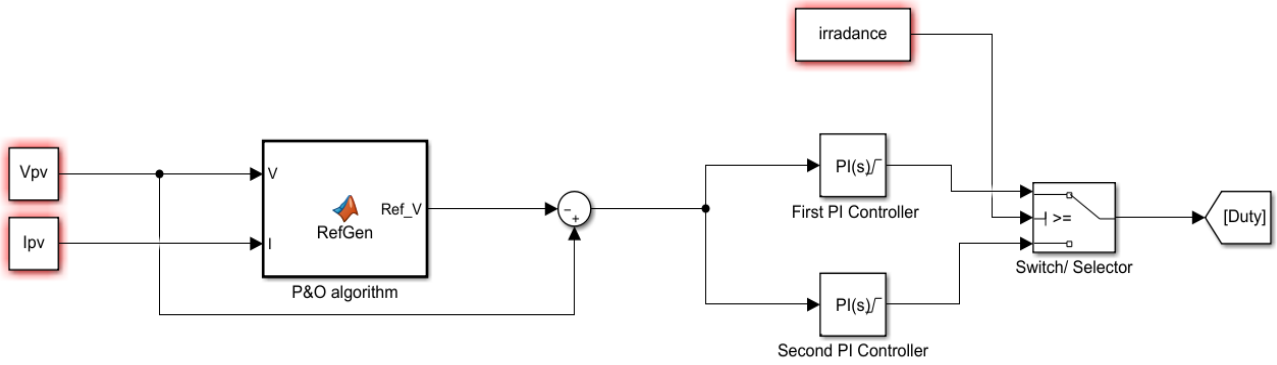

Figure 16.control circuit using two PI Controllers

The reason for using the PI controller is that it eliminates the steady-state error that is excited with the proportional controller only (Liuping Wang., 2020). The error signal from the P&0 algorithm is multiplied by two terms to produce the control law of the DC-DC boost converter, as shown in the following equation.

$$u(t) = k_p e(t) + k_i \int_0^t e(t)\, dt \qquad (2.29)$$

Where k_p and k_i are the proportional and integral gains, automatic tuning is the most appropriate way to choose these gains; hence a good performance from the PV system can be achieved. The automatic tuning has been done using the properties of the two PI controllers, built-in MATLAB Simulink. for the first PI, setting the input irradiance swing between 500 to 1000 and a step control signal has been applied to the plant. After the simulation time is finished, the output response and the appropriate gains can be obtained, as shown in figure 17.

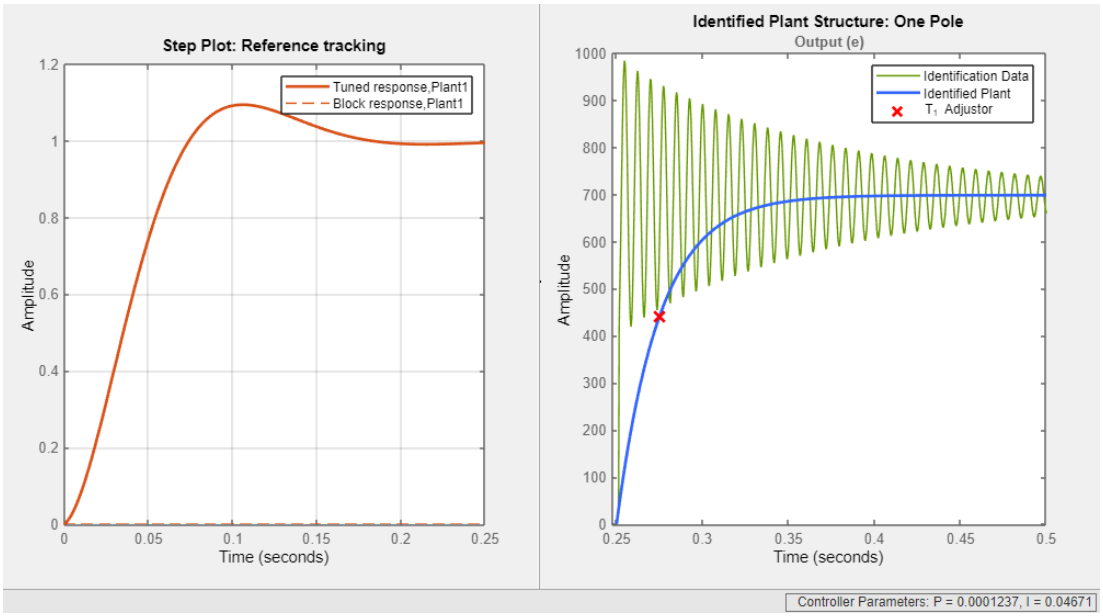

Figure 17.controller Parameters (Gains) for the first PI controller

This process will be repeated with the second PI controller, but the input irradiance is less than 500. After testing all the possible gains of both controllers, table 3 represents the appropriate gains for this project.

Table 3.the gains of the proposed PI controllers

Parameter	1st PI	2st PI
k_p	0.0001	0.00055
k_i	0.05	0.001

After modelling the whole system, figure 18 shows the implemented block of the maximum power point tracking system in MATLAB Simulink.

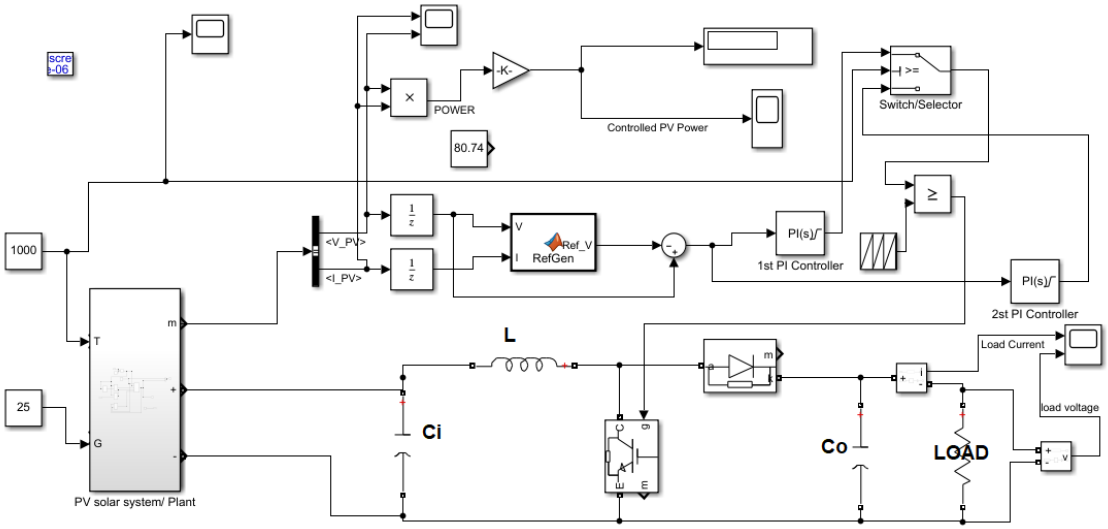

Figure 18.block diagram of the proposed system

3 Result

3.1 First scenario (variable irradiance and constant temperature)

In this scenario, the temperature has been fixed at 25 c^0; however, the sun intensity is changed to test the proposed framework's response. Figures (19-20-21) show the output power of the solar panel system when the irradiance is equal to 1000, 800,400 W/m^2.

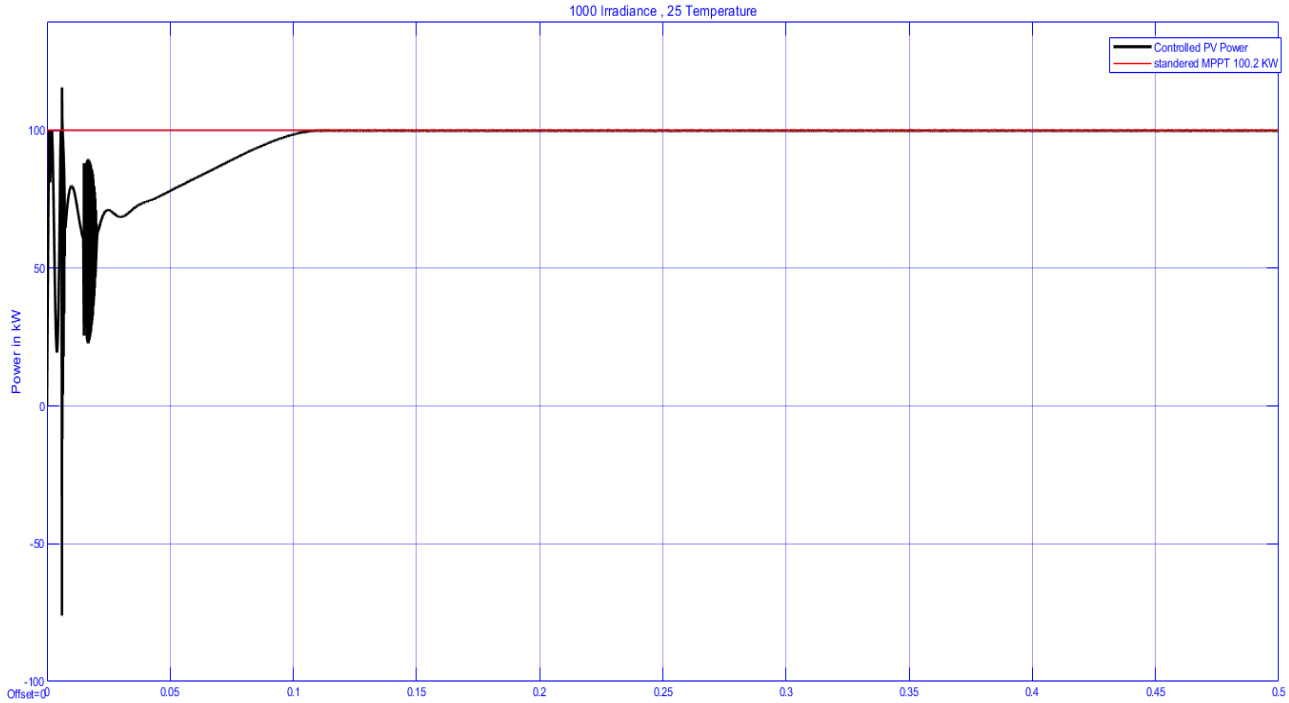

Figure 19.power performance when the Irradiance = 1000 and T =25 c^0

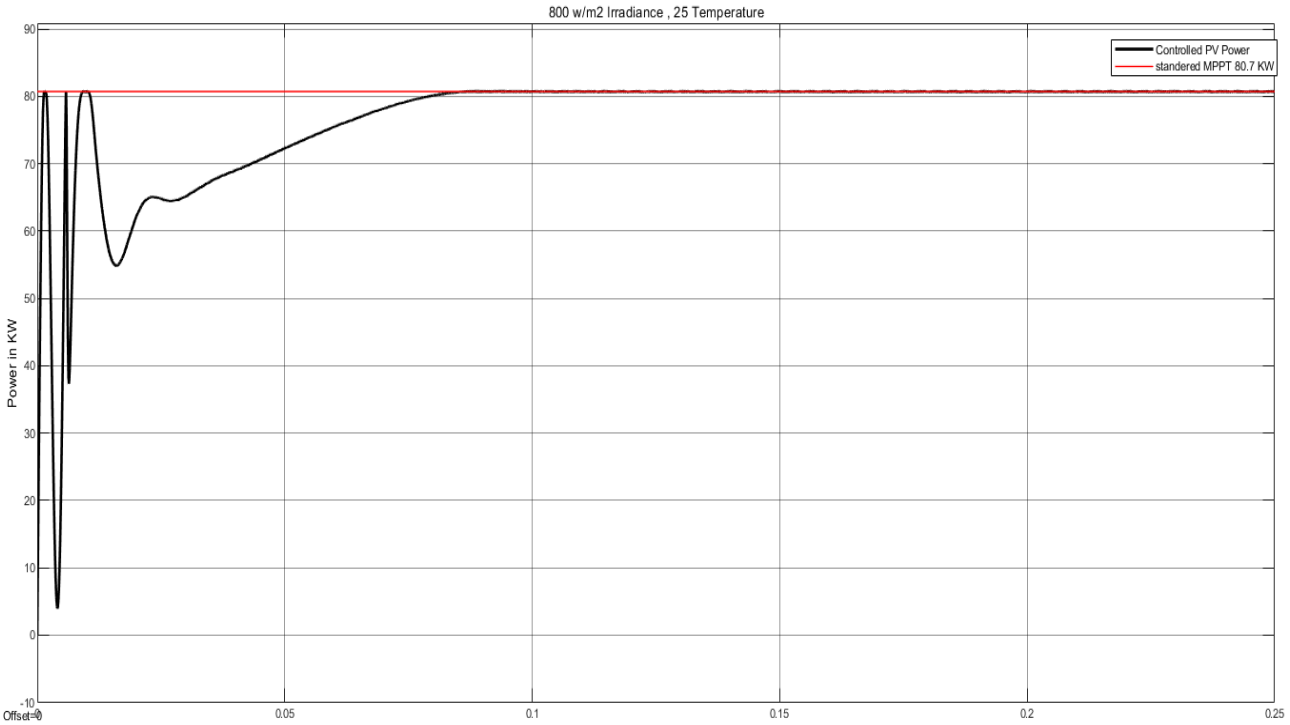

Figure 20.power performance when the Irradiance = 800 W/m^2 and T =25 c^0

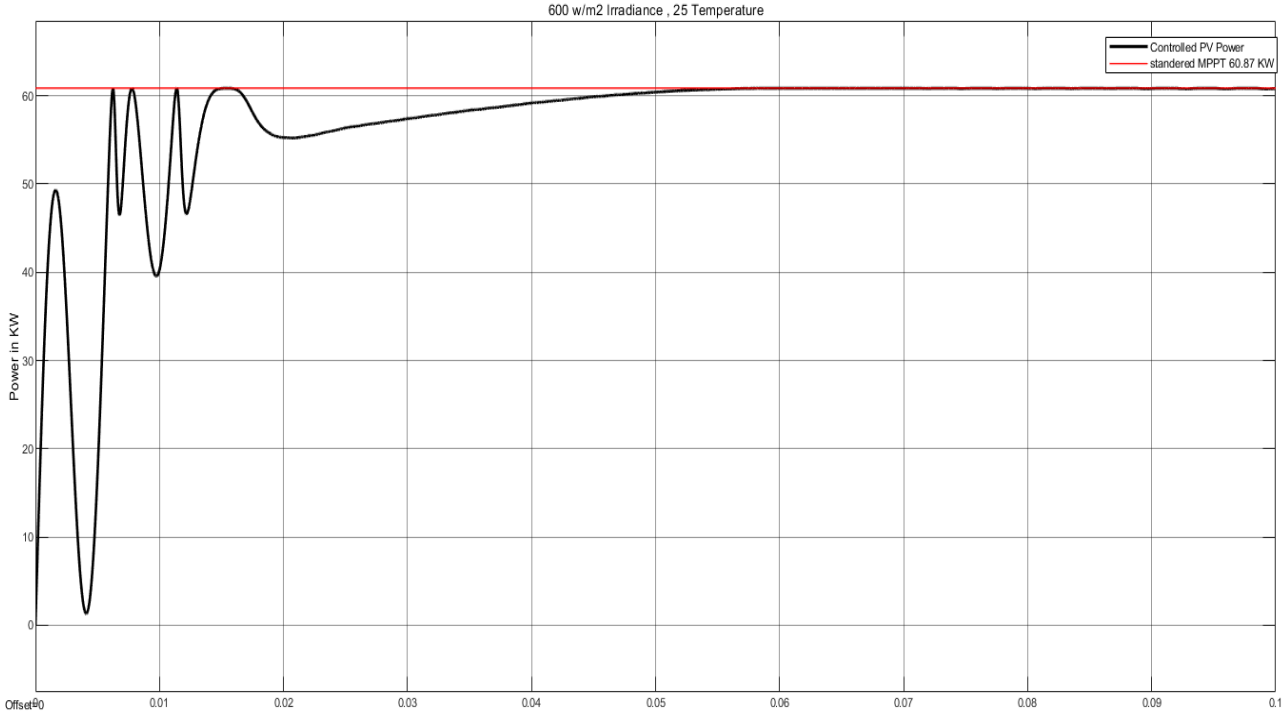

Figure 21.PV power performance when the Irradiance = 600 W/m^2 and T =25 c^0

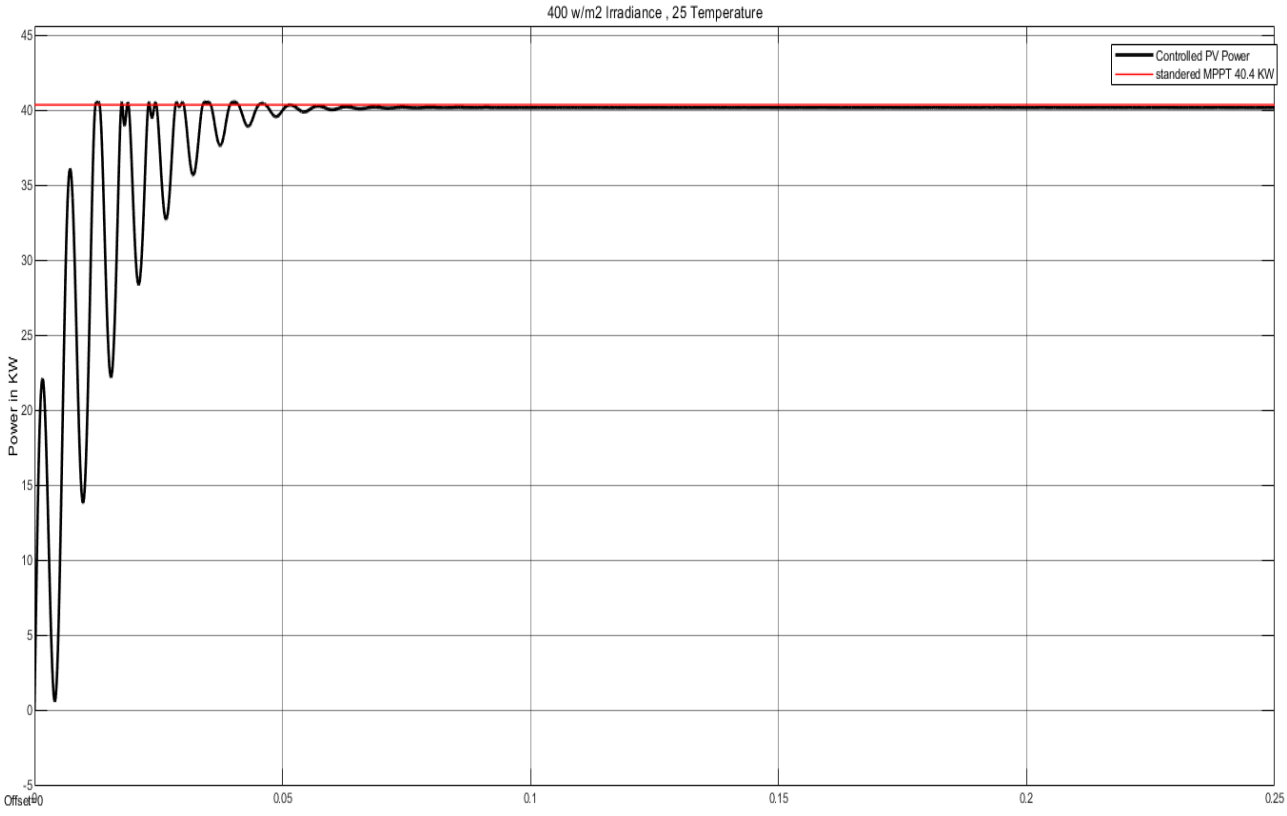

Figure 22.PV power performance when the Irradiance = 400 W/m^2 and T =25 c^0

The following figures (23-24) illustrate the behaviour of the PV voltage and current under 900 and 600 W/m^2 and constant temperature 25 c^0.

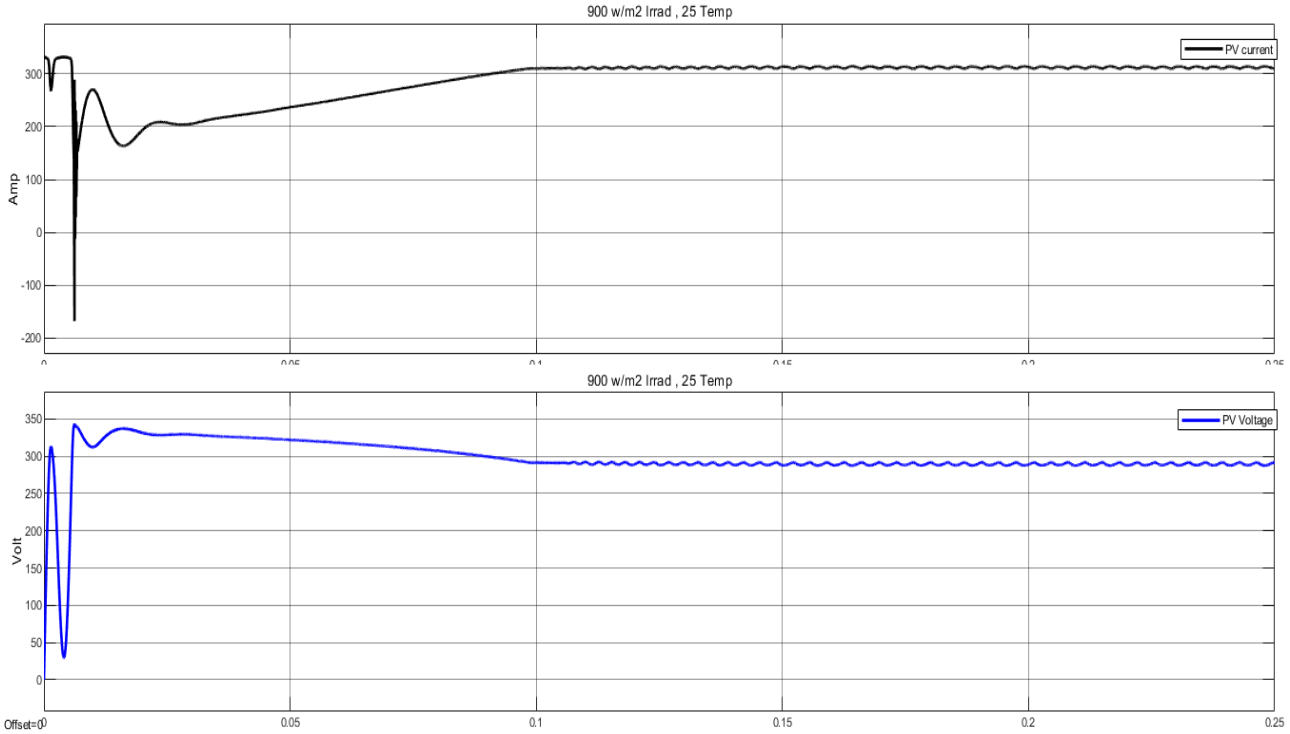

Figure 23.PV voltage and current when the Irradiance = 900 W/m^2 and T =25 c^0

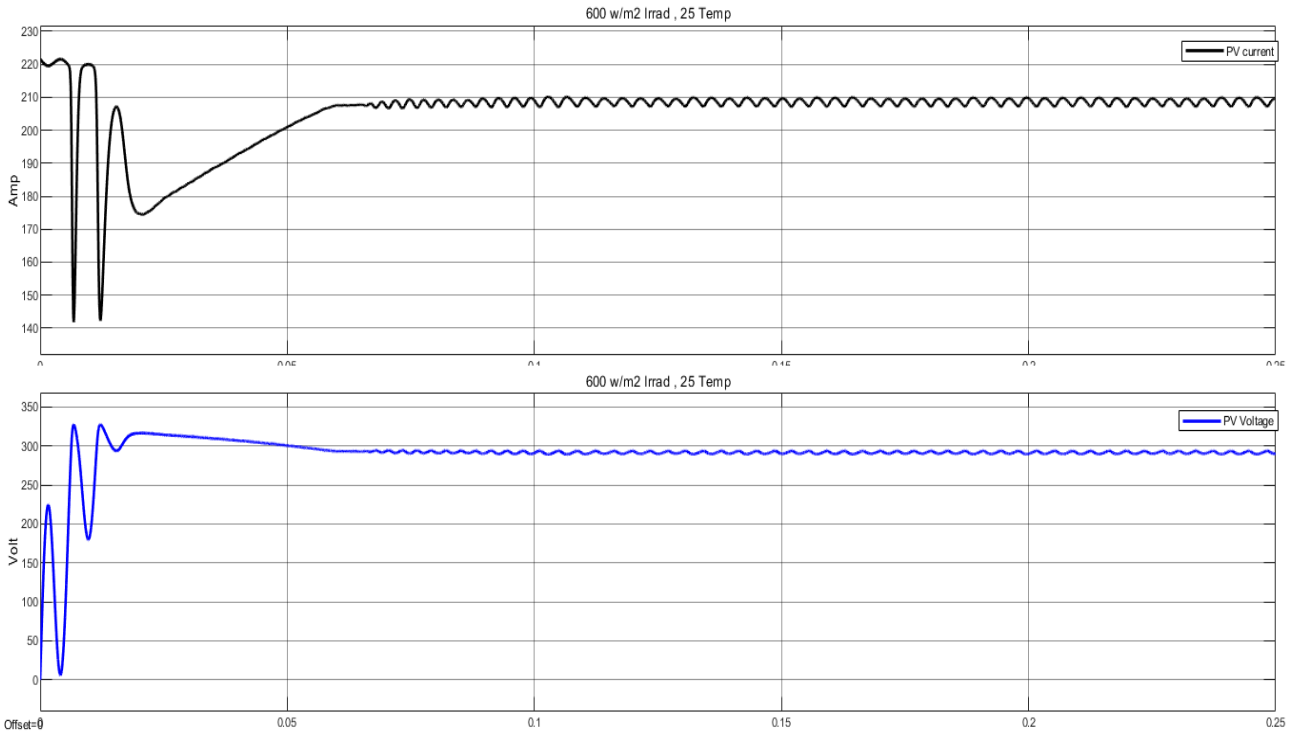

Figure 24.PV voltage and current when the Irradiance = 600 W/m^2 and T =25 c^0

The voltage and the current across the load can be represented in figures (25-26) when the irradiance is 800 and 400 W/m^2.

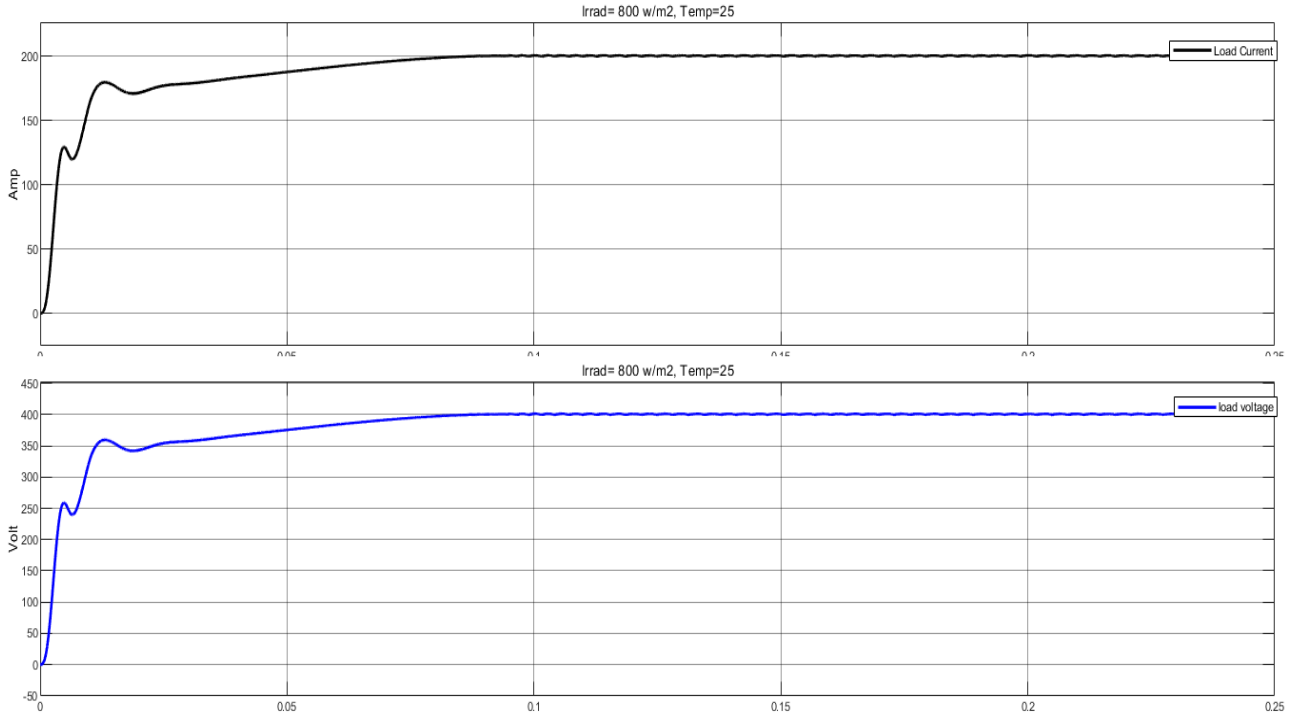

Figure 25.Load voltage and current when the Irradiance = 400 W/m^2 and T =25 c^0

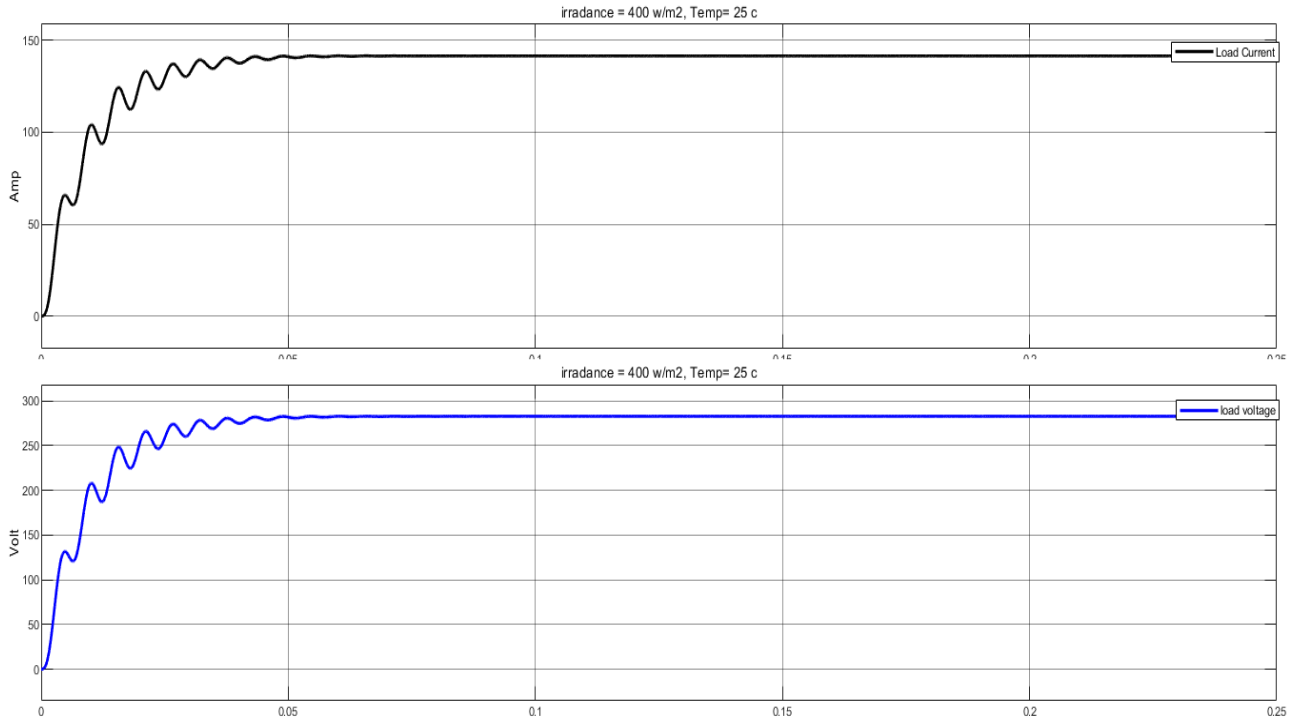

Figure 26.Load voltage and current when the Irradiance = 400 W/m^2 and T =25 c^0

Figures (27-28) show the efficiency of the proposed system for tracking the maximum power point when the irradiance equals 800 and 400.

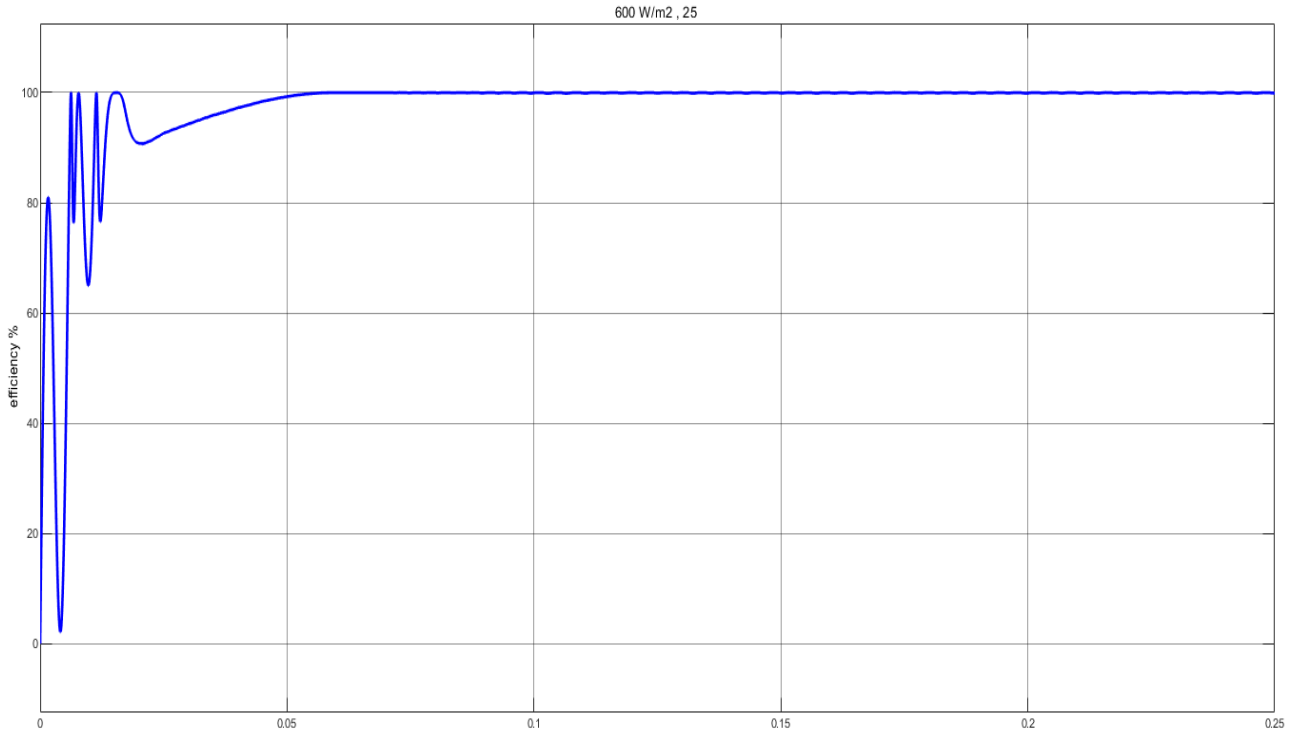

Figure 27.the efficiency of the system when the Irradiance = 600 W/m^2 and T =25 c^0

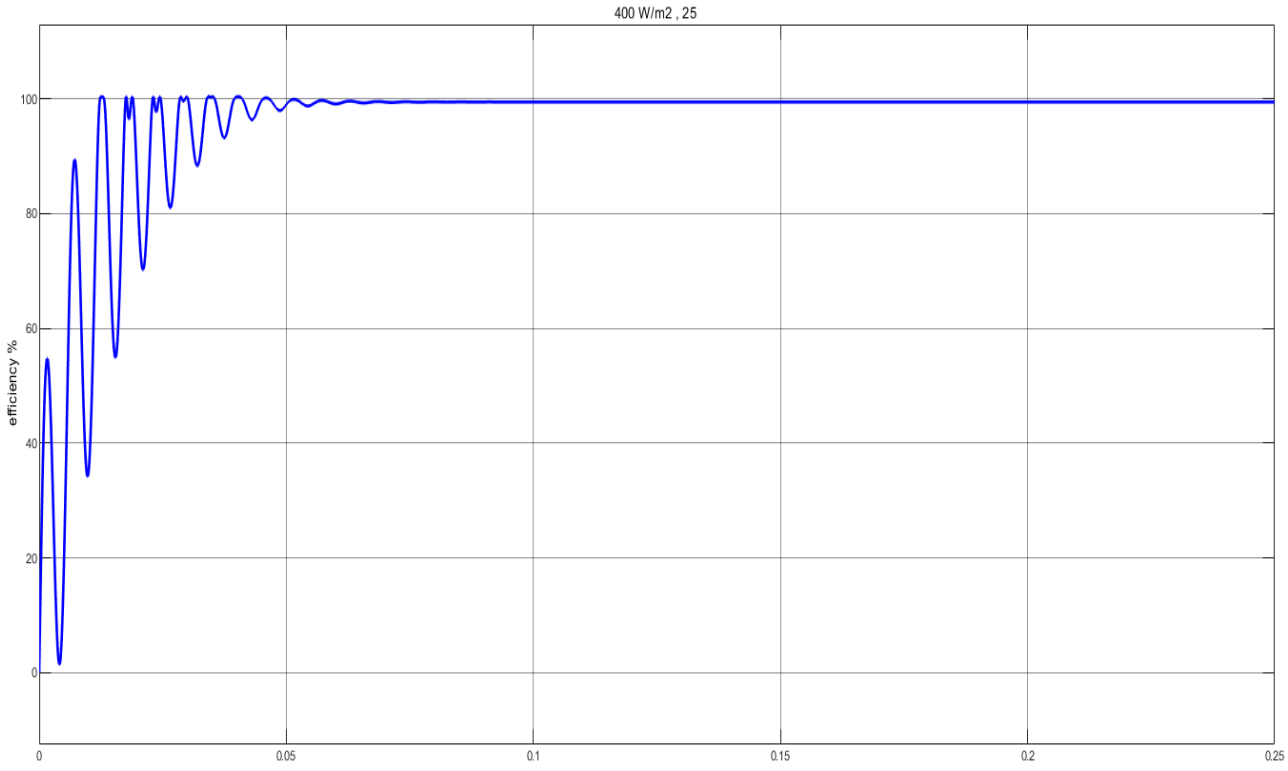

Figure 28.the efficiency of the system when the Irradiance = 400 W/m^2 and T =25 c^0

3.2 Second scenario (variable temperature and constant irradiance)

The second scenario tested the system under different temperatures with constant sun intensity (1000 W/m^2). Figures (29-30) show the output power of the solar panel system when the temperature is 45,10 c^0, and 1000 W/m^2 radiation.

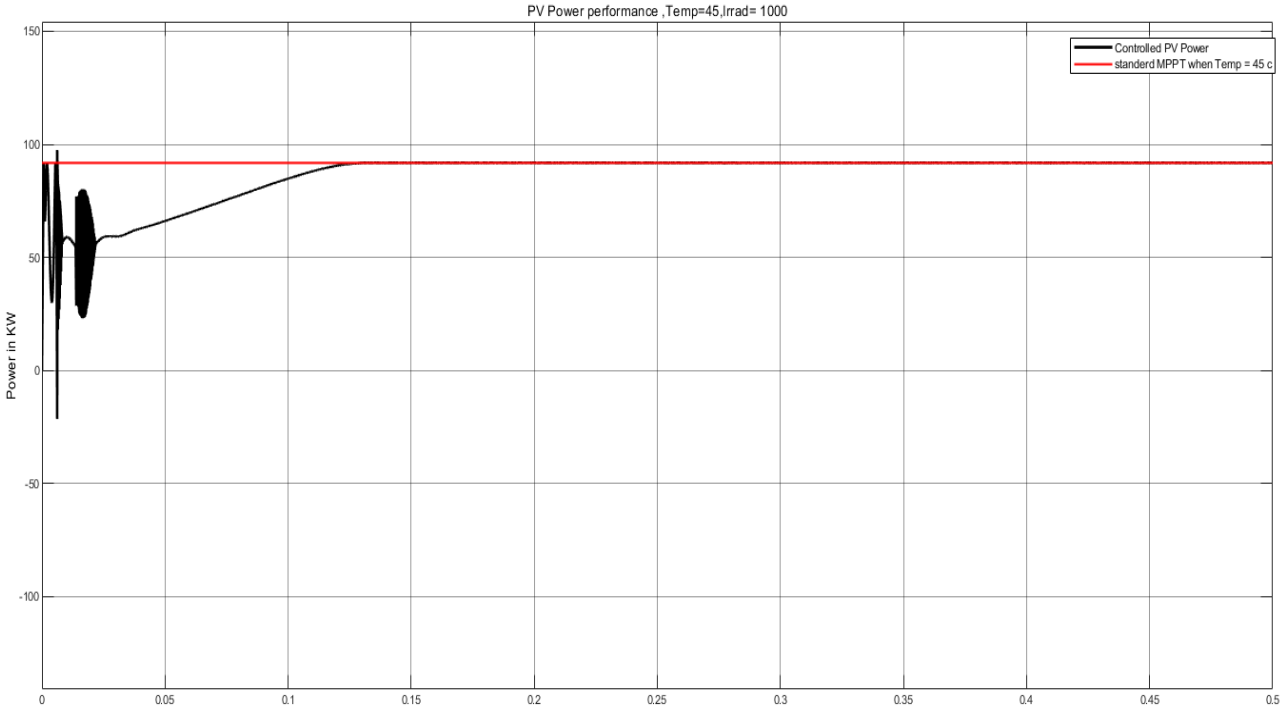

Figure 29.power performance when the temperature =45 $c^0$and Irradiance=1000 W/m^2

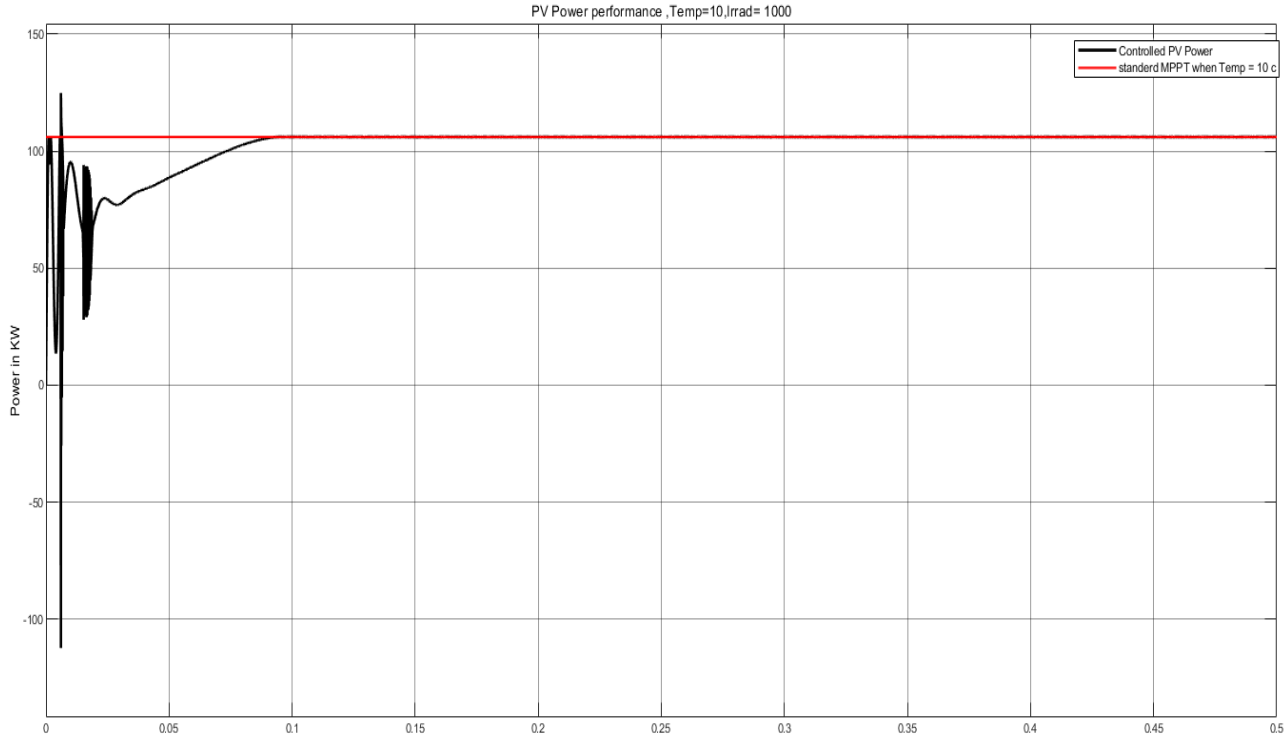

Figure 30.power performance when the temperature =10 $c^0$and Irradiance=1000 W/m^2

Furthermore, figures (31-32) show the voltage-current characteristics of the solar panel system and the load under the same conditions mentioned in the previous paper.

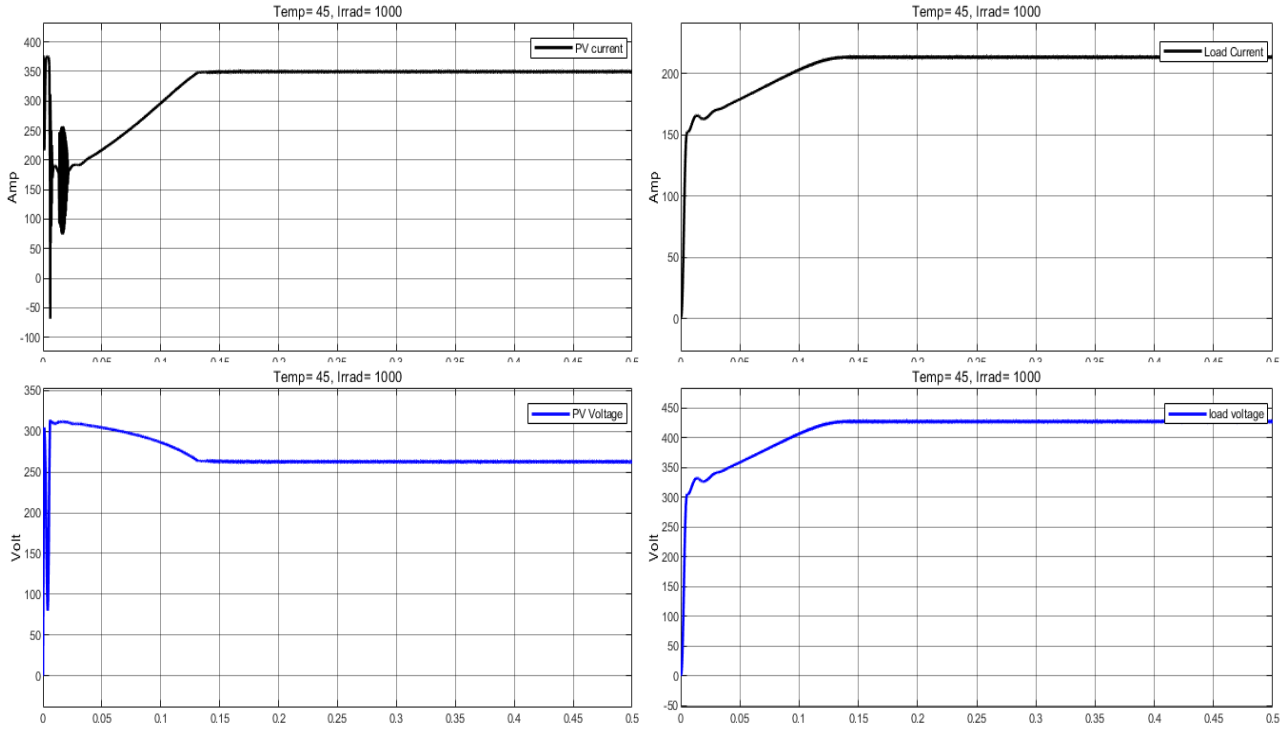

Figure 31.I-V characteristics of the PV System and load when T =45 $c^0$and irradiance = 1000 W/m^2

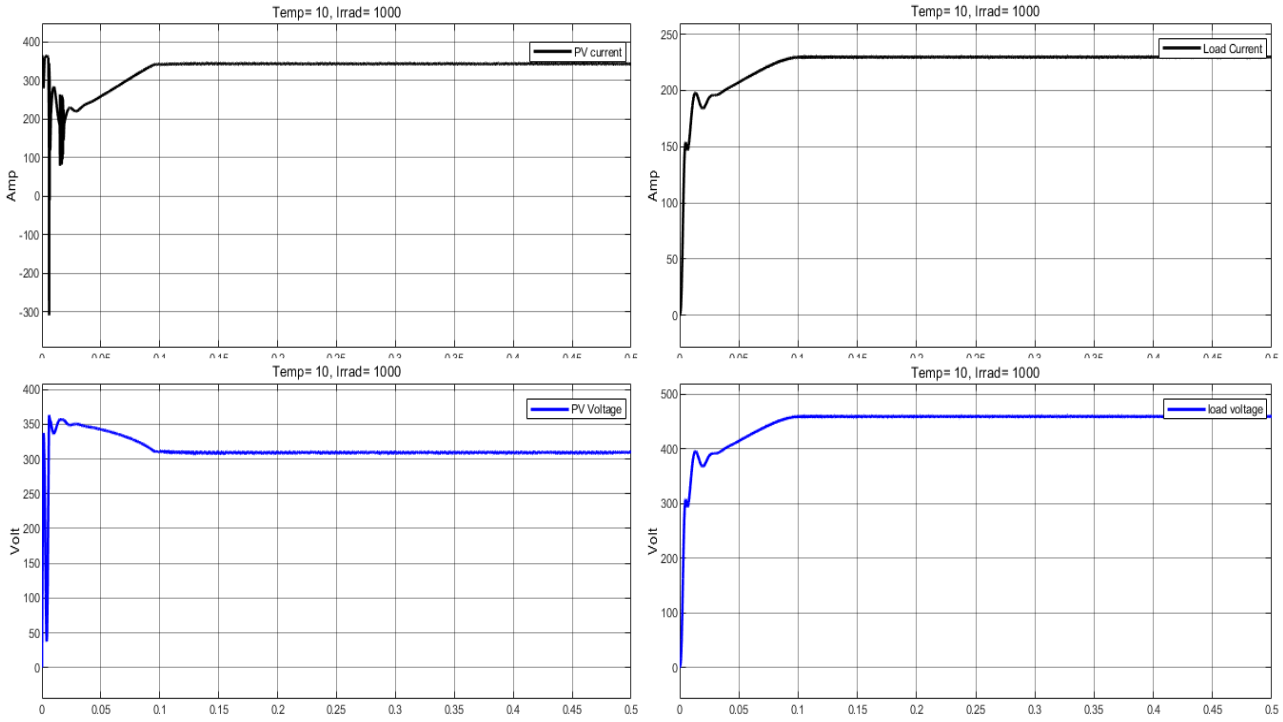

Figure 32.I-V characteristics of the PV System and load when T =45 $c^0$and irradiance = 1000 W/m^2

The efficiency of the proposed system in the second scenario can be represented in figures (33-34). Note that the temperature has been chosen equal to 35 and 25 c^0 with constant irradiance of 1000 W/m^2.

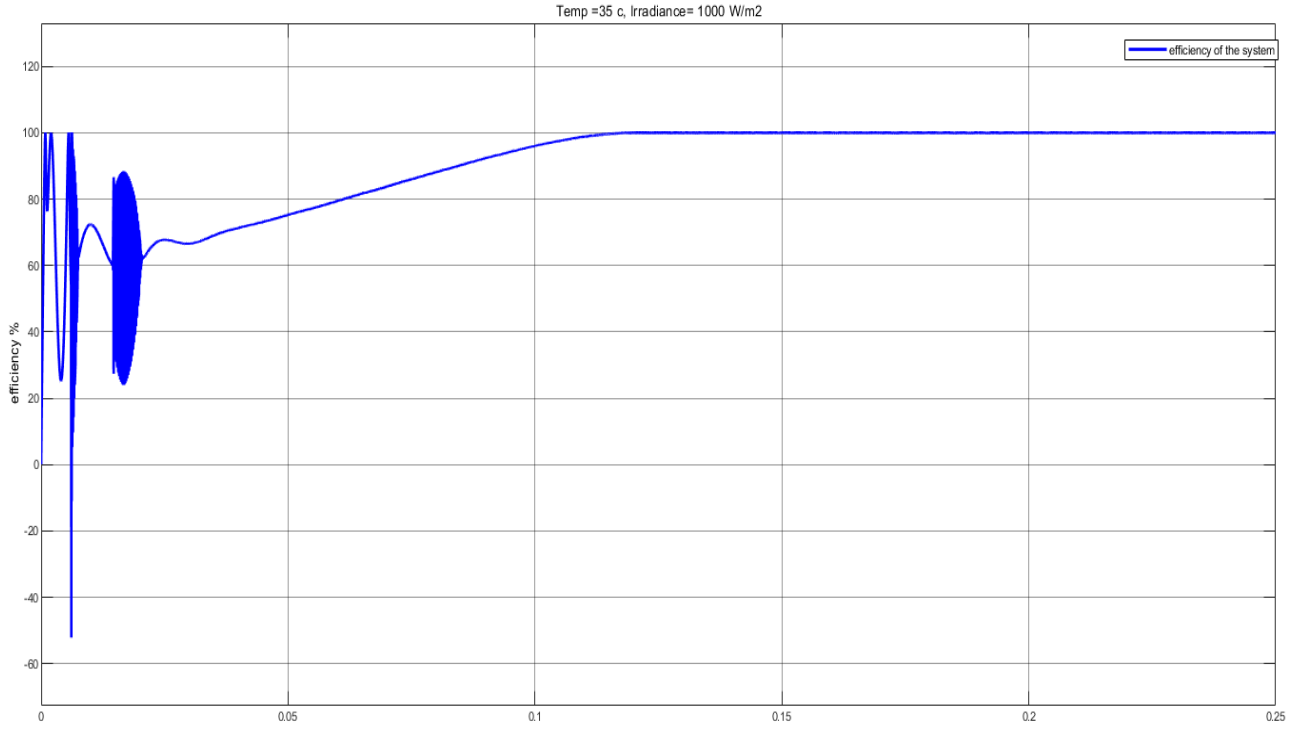

Figure 33.the efficiency of the system when T =35 c^0 and Irradiance =1000 W/m^2

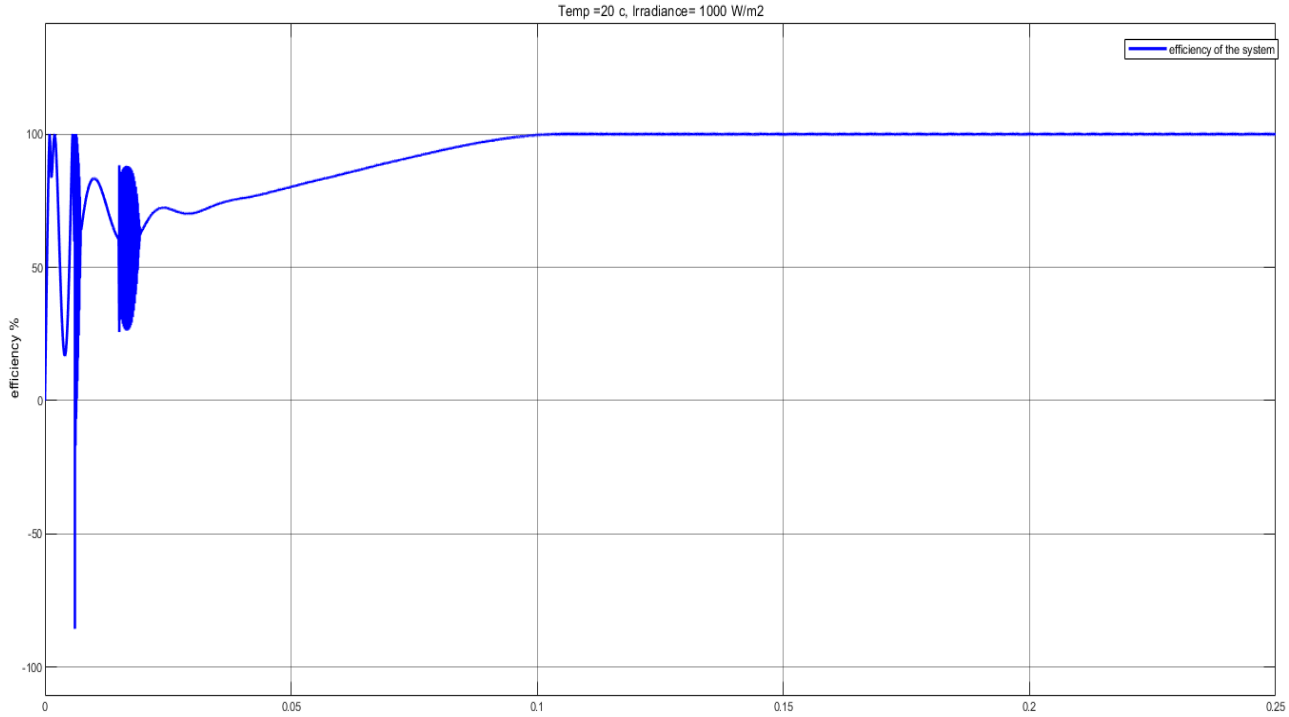

Figure 34.the efficiency of the system when T =20 $c^0$and Irradiance =1000 W/m^2

3.2 comparison between the proposed system and other methods.

The most common method to check the system's performance is the comparison with other techniques done by others. Figures (35-36-37) compare the proposed framework's power performance and efficiency with the PWM method.

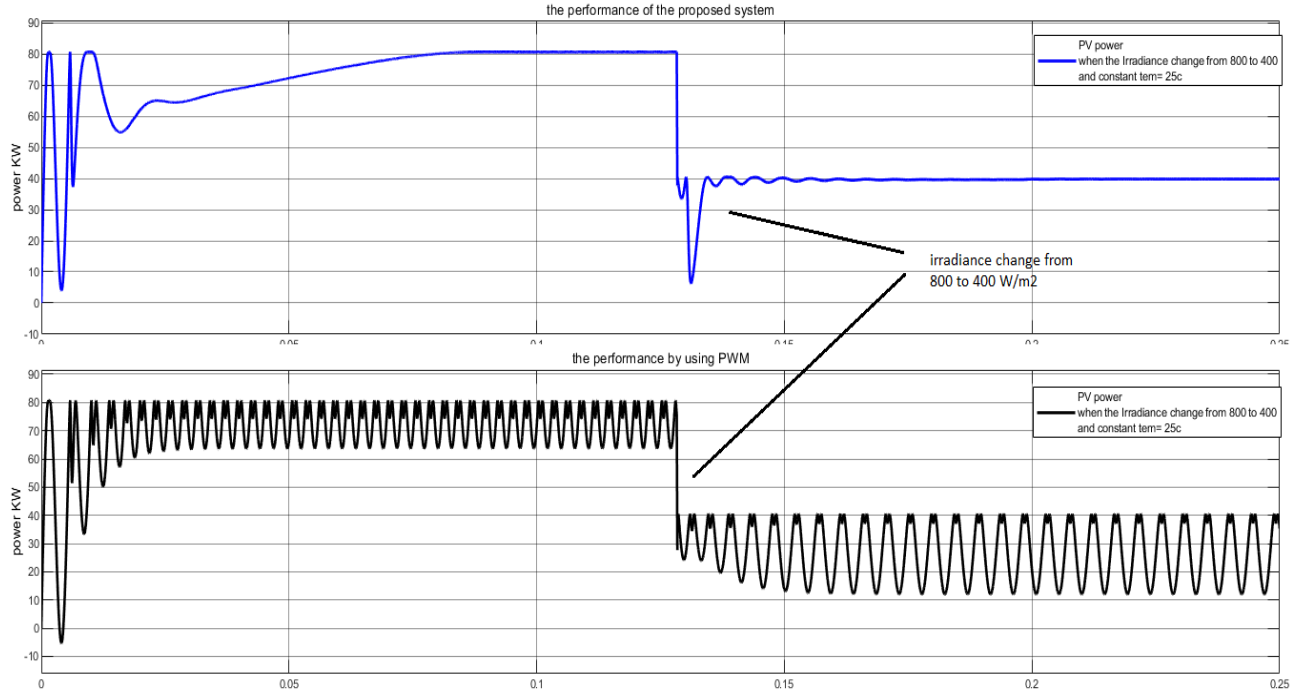

Figure 35.comparison between the power performance of the proposed method and the PWM method (variable irradiance and constant temperature)

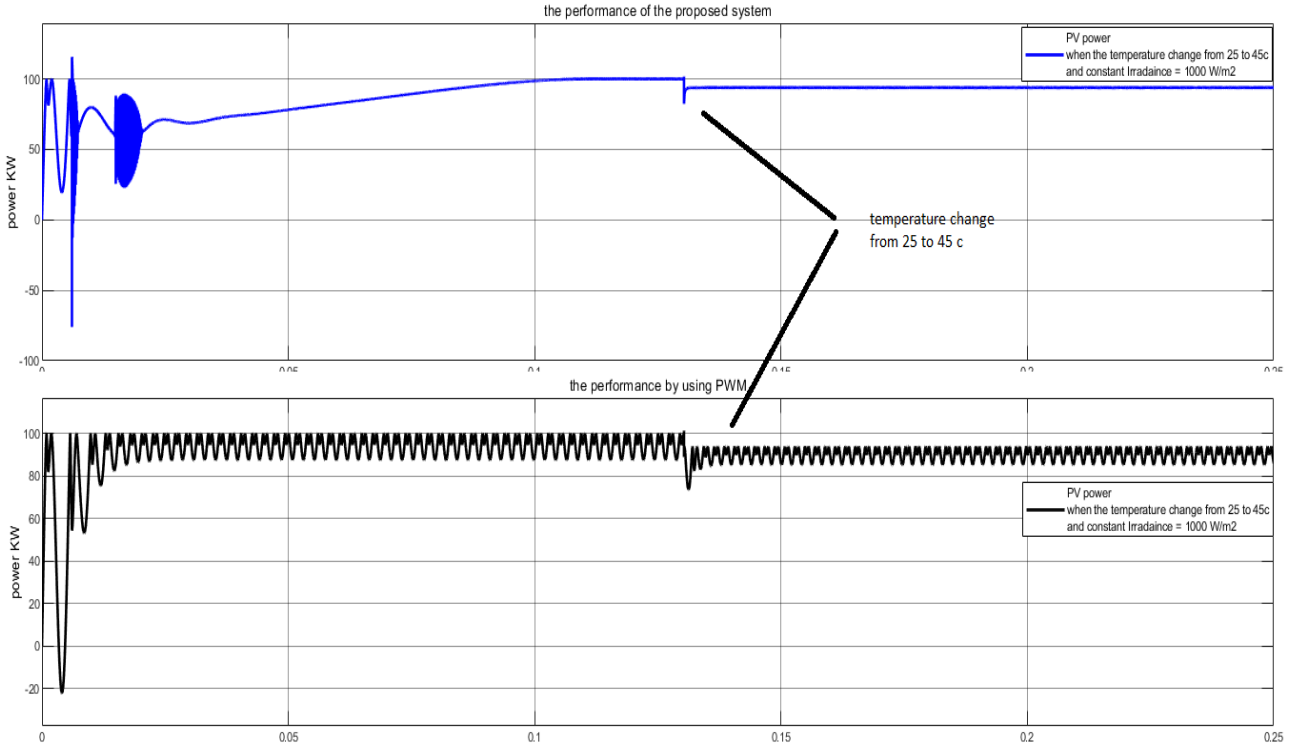

Figure 36.comparison between the power performance of the proposed method and the PWM method (variable temperature and constant irradiance)

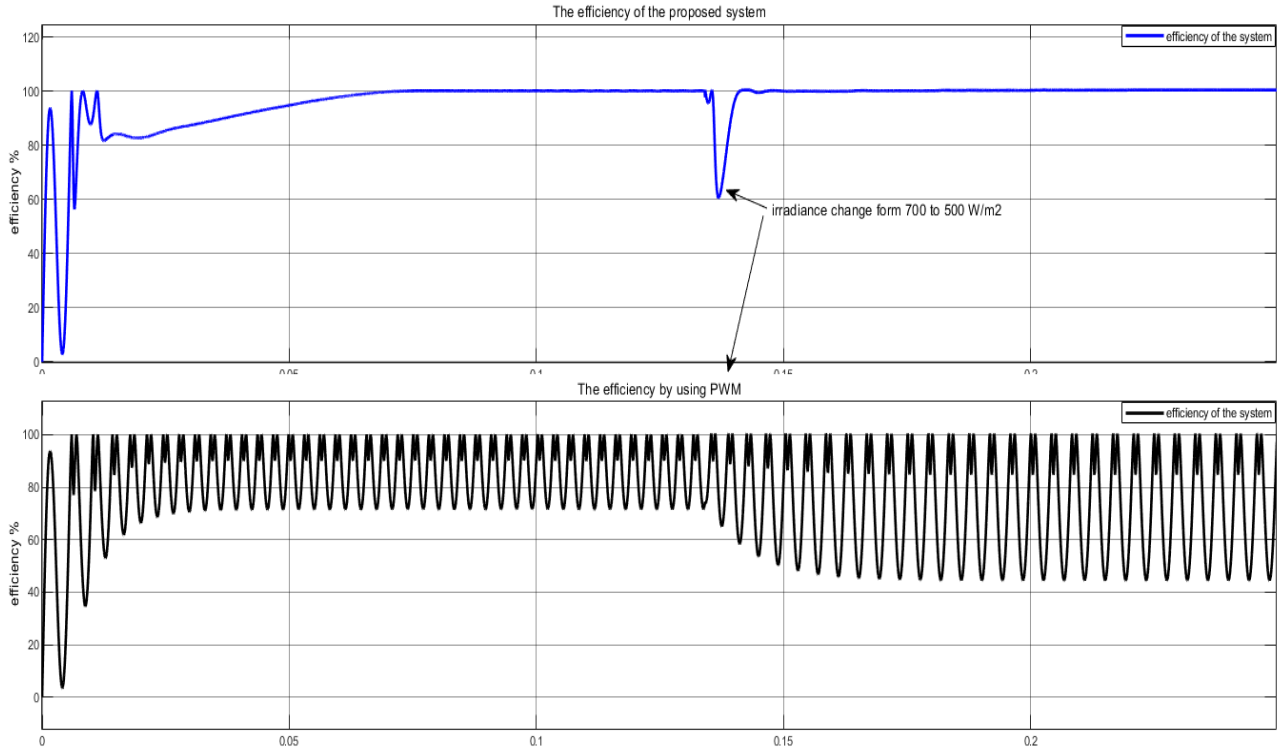

Figure 37.comparison between the efficiency of the proposed method and the PWM method (variable irradiance and constant temperature)

Furthermore, Figures (38-39-40) compare the proposed framework's power performance and efficiency with another method named (incremental algorithm and one PI controller).

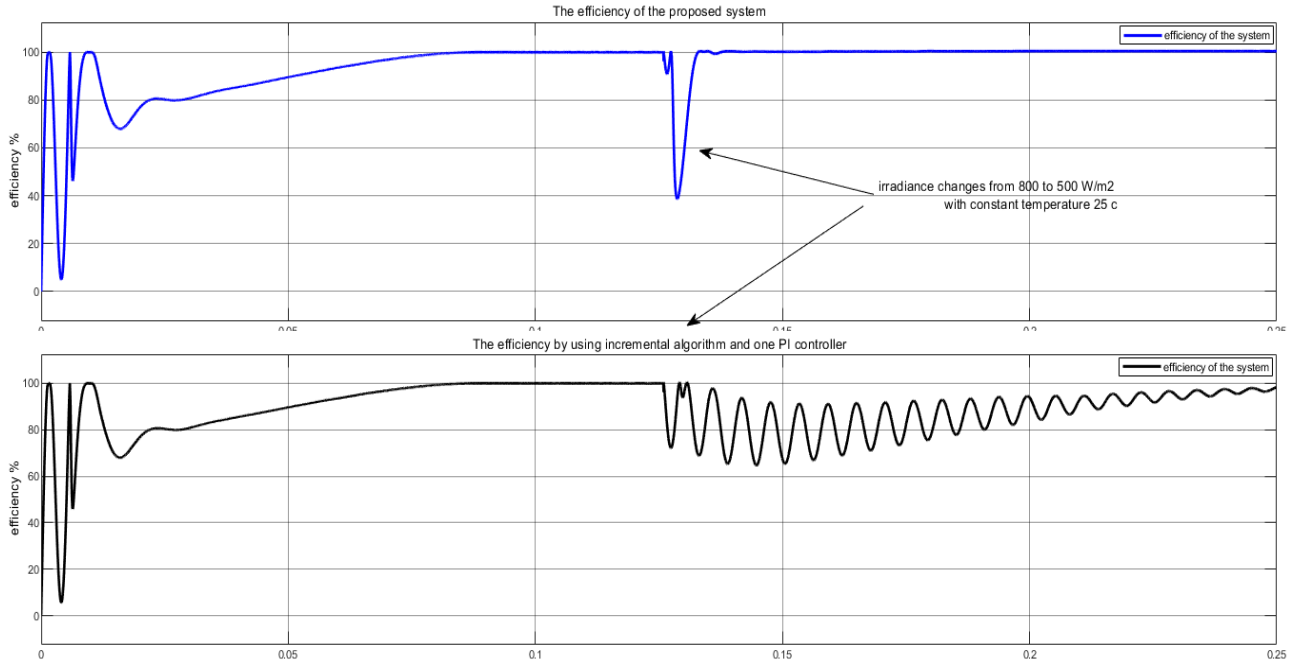

Figure 38.comparison the PV power performance of the proposed method and the (incremental + one PI controller) method (variable temperature and constant irradiance)

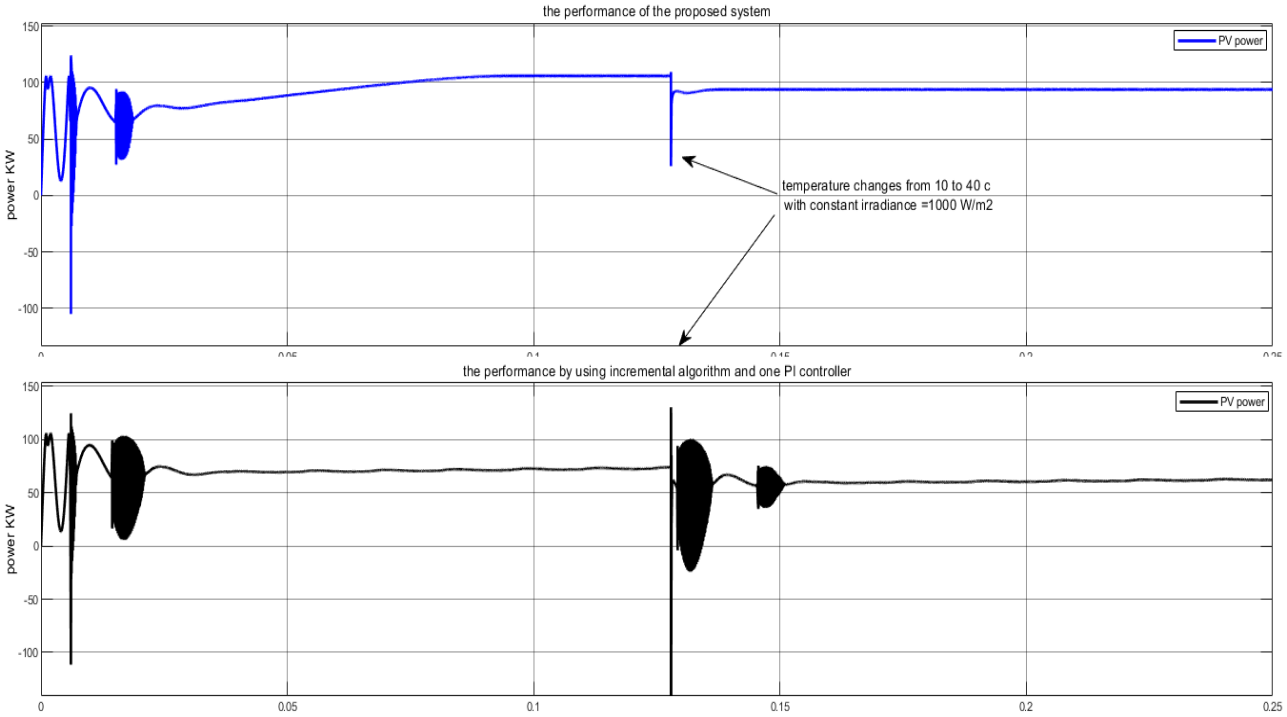

Figure 39.comparison between the power performance of the proposed method and the (incremental + one PI controller) method (variable temperature and constant irradiance)

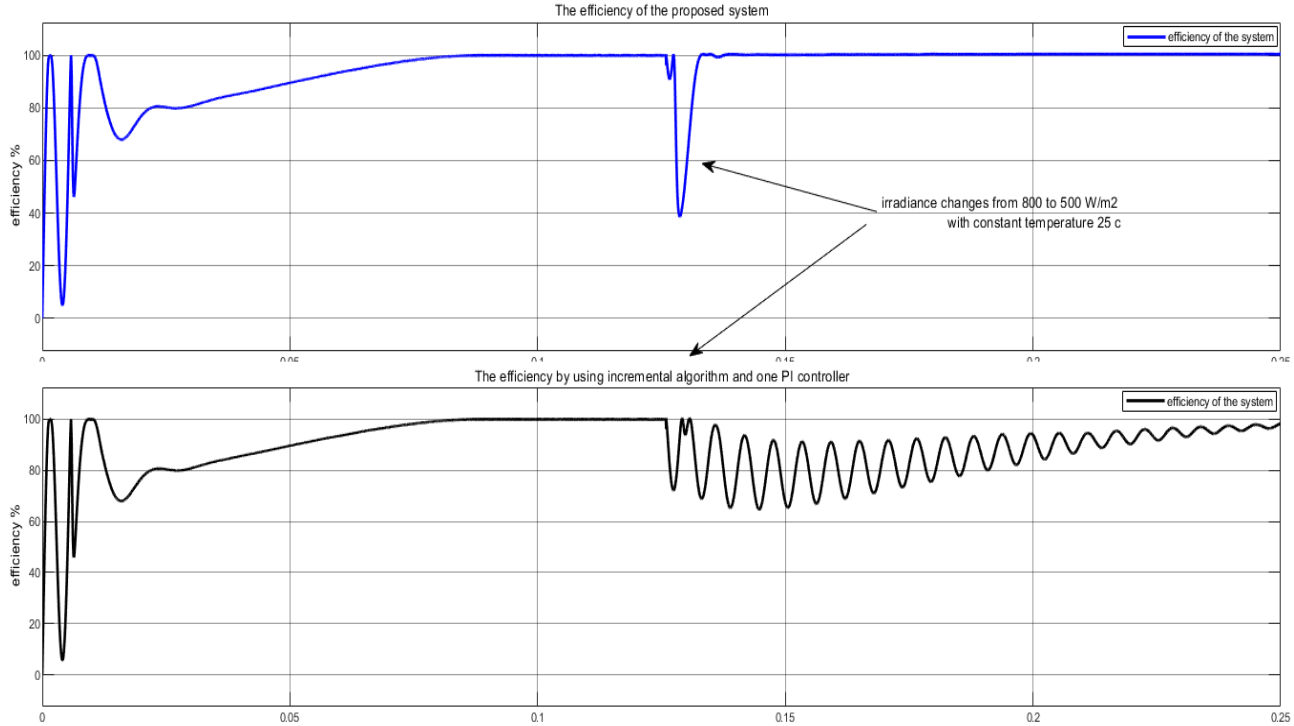

Figure 40.comparison between the efficiency of the proposed method and the (incremental + one PI controller) method (variable irradiance and constant temperature)

4 Discussion

The results mentioned above showed that the system did well. In the first scenario, the PV power observed the typical maximum power points given in Figure (7) under different conditions. For example, when the radiation was equal to 1000 W/m^2 in Figure (19), the solar system's power equalled 100.2 kilowatts. Similarly, Figures (20) and (22) show that when the irradiance is set at 800 and 400 W/m^2, the power of the proposed solar system equals 80.78 and 40.45 kilowatts, respectively. Concerning the voltage and current characteristics of the solar system, the results showed that when the radiation was equal to 900 W/m^2, from figure (23), the values of the voltage and current of the solar panel were equal to 400 volts and 150 amps, respectively. These are precisely the same as the desired characteristics given in Figure (7) at the set conditions.

In terms of load I-V characteristics, the results showed that after the setting time, they stabilized at constant values without fluctuation, as shown in Figures (25 -26), due to the presence of the capacitor at the output side of the DC-DC boost converter. According to the system's efficiency, the results proved, as shown in figures (27-28), that the efficiency of the proposed system is exceptionally high, which indicates that the error between the solar system's power and the desired maximum power (standards given in figure 7) is zero under different conditions. The credit is due to the use of the PI controller, which always makes the steady state error as low as possible. To illustrate the performance of the proposed system in the first scenario (variable irradiance and constant temperature). Table 4 shows the PV power, voltage, and current under different conditions.

Table 4. the results of the first scenario

Irradiance in $\mathbf{W}/\boldsymbol{m^2}$	Temperature in $\boldsymbol{c^0}$	Power in kilowatts	Voltage in volt	Current in amps	Desired power	Desired voltage	Desired current	efficiency %
1000	**25**	**100.2**	**290**	**345**	**100.2**	**290**	**345**	**100**
900	**25**	**90.46**	**289.6**	**312**	**90.46**	**289.6**	**312**	**100**
800	**25**	**80.78**	**292**	**276.6**	**80.78**	**292**	**276.6**	**100**
700	**25**	**70.87**	**292.6**	**242.2**	**70.87**	**292.6**	**242.2**	**100**
600	**25**	**60.87**	**293.3**	**207.5**	**60.87**	**293.3**	**207.5**	**100**
500	**25**	**50.75**	**293.3**	**173**	**50.75**	**293.3**	**173**	**100**
400	**25**	**40.4**	**290.7**	**139**	**40.4**	**290.7**	**139**	**100**

In the second scenario (variable temperature and constant irradiance), The results showed that the performance of the proposed system also did significantly well. For instance, in figures (29-30), the PV power appropriately tracked the desired maximum power points given in figure (8) when the temperature was set at 45 and 10. Similar to the first scenario, The I-V characteristics of the designed solar panel system and the load achieved their typical values, as shown in figures (31-32). Regarding the proposed system's efficiency, figures (33-34) illustrated that 100% efficiency had been obtained under given conditions.

Table (5) introduces the P-V and I-V characteristics of the proposed MPPT. From both scenarios, the current seems more affected by the change in the irradiance, while in table 5, the voltage was more sensitive to temperature disturbance.

Table 5.the results of the second scenario

Irradiance in $\mathbf{W}/\boldsymbol{m^2}$	Temperature in $\boldsymbol{c^0}$	Power in kilowatts	Voltage in volt	Current in amps	Desired power in kilowatts	Desired Voltage In volt	Desired current In amps	efficiency %
1000	**40**	**93.9**	**270**	**347.9**	**93.3**	**270**	**347.9**	**100**
1000	**35**	**95.99**	**276.6**	**347.1**	**95.99**	**276.6**	**347.1**	**100**
1000	**30**	**98.05**	**283.2**	**346.3**	**98.05**	**283.2**	**346.3**	**100**
1000	**25**	**100.2**	**290**	**345.4**	**100.2**	**290**	**345.4**	**100**
1000	**20**	**102**	**296.8**	**344**	**102**	**296.8**	**344**	**100**
1000	**15**	**104**	**303.4**	**343.1**	**104**	**303.4**	**343.1**	**100**
1000	**10**	**106**	**310.2**	**342**	**106**	**310.2**	**342**	**100**

Regarding the accuracy of the proposed system, some comparisons have been made with methods used by other researchers for more validation. Figures (35-37) compared the proposed system's performance with the results obtained using the pulse width modulator. In figure 35 (blue line), the power of the designed solar system tracked the typical MPP without any oscillation while it swayed around the equilibrium point, as shown in figure 35 (black line). In terms of disturbance rejection, the result showed that for any sharp change in the external conditions, the proposed system tracked the steady state values faster than the other. For instance, in figure 36 (blue line), the new MPP was achieved within a millisecond when the temperature was changed sharply from 25 to 45 c. This rejection did not happen during the PWM method shown in the black line. Besides, 100 % efficiency had been achieved for the proposed method, while it was not for the other, as stated in figure 37.

Another comparison was made with a method that used one PI controller. The results proved that the performance of the proposed system was better, faster and more efficient, as given in figures (38-39). The problem with using one PI controller has been solved. As shown in figure 38 (blue line), the maximum power was achieved appropriately when the irradiance was changed from 700 to 500 w/m2. That was the effect of tuning two PI controllers while one PI controller was not enough to respond to all disturbances, as shown in figure 38 (black line).

Experimentally, this proposed framework can be installed and applied easily in daily usage. However, the limitation of this project is that partial shading has not been considered for checking the performance of the proposed system because it has more than one peak; therefore, the perturb and observe algorithm is insufficient to track the maximum one.

5 Conclusion

In conclusion, this project has successfully implemented the MPPT system under different conditions. For both scenarios, the proposed system appropriately tracks the maximum power. The novelty of this design improves the system's performance (efficiency, speed, and oscillation) compared with previous methods. In addition, the system's controllability, observability, and stability have been satisfied. In the real world, this design can be implemented and applied in daily life, such as a battery charge controller. However, this project does not consider partial shading because it has more than one MPP; therefore, advanced control techniques are needed to solve this problem. As a recommendation, this framework could be connected with artificial intelligence techniques to overcome the drawbacks of partial shading.

References

Abd El-Basit, Wafaa & El–MAKSOOD, Ashraf & Soliman, Fouad. (2013). Mathematical Model for Photovoltaic Cells. Leonardo Journal of Sciences. 12. 13-28.

Anon, 2021. System Stability. Available at: https://eng.libretexts.org/@go/page/24396 [Accessed August 15, 2022].

Anto, Emmanuel & Asumadu, Johnson & Okyere, Philip. (2016). PID control for improving P&O-MPPT performance of a grid-connected solar PV system with Ziegler-Nichols tuning method. 1847-1852. 10.1109/ICIEA.2016.7603888.

Anoop, K. and Nandakumar, M., 2018, January. A novel maximum power point tracking method based on particle swarm optimization combined with one cycle control. In 2018 International Conference on Power, Instrumentation, Control and Computing (PICC) (pp. 1-6). IEEE.

Baimel, D., Tapuchi, S., Levron, Y. and Belikov, J., 2019. Improved Fractional Open Circuit Voltage MPPT Methods for PV Systems. Electronics, 8(3), p.321.

Barrow, E.M. and Hulme, M., 1996. Changing probabilities of daily temperature extremes in the UK related to future global warming and changes in climate variability. Climate Research, 6(1), pp.21-31.

Chen, Y., Ahn, H.S. and Xue, D., 2006. Robust controllability of interval fractional order linear time invariant systems. Signal Processing, 86(10), pp.2794-2802.

Dabra, V., Paliwal, K., Sharma, P. and Kumar, N., 2017. Optimization of photovoltaic power system: a comparative study. Protection and Control of Modern Power Systems, 2(1).

Fuentes, S., Villafafila-Robles, R., Olivella-Rosell, P., Rull-Duran, J. and Galceran-Arellano, S., 2020. Transition to a greener Power Sector: Four different scopes on energy security. Renewable Energy Focus, 33, pp.23-36.

Gandomkar, A., Parastar, A. and Seok, J.K., 2016. High-power multilevel step-up DC/DC converter for offshore wind energy systems. IEEE Transactions on Industrial Electronics, 63(12), pp.7574-7585.

Hussein Selman, N., 2016. Comparison Between Perturb & Observe, Incremental Conductance and Fuzzy Logic MPPT Techniques at Different Weather Conditions. International Journal of Innovative Research in Science, Engineering and Technology, 5(7), pp.12556-12569.

Kashif I., Zaina of Photovoltaic (PV) Modules Using Differential Evolution (DE), Science-Direct, Solar Energy, Elsevier Ltd., 2011, 85, p. 2349–2359.

Kumari, J.S., Babu, D.C.S. and Babu, A.K., 2012. Design and analysis of P&O and IP&O MPPT techniques for photovoltaic system. International Journal of Modern Engineering Research, 2(4), pp.2174-2180.

Li, H., Wang, J. and Meng, J., 2021. Chapter 4 - Nonlinear control. In: D. Zhang and B. Wei, ed., Learning Control. [online] pp. 93-102. Available at: <https://doi.org/10.1016/B978-0-12-822314-7.00009-2> [Accessed 16 August 2022].

Liuping Wang., 2020. PID Control System Design and Automatic Tuning Using MATLAB/Simulink. Wiley-IEEE Press.

Murtaza, A.F.; Sher, H.A.; Chiaberge, M.; Boero, D.; Giuseppe, M.D.; Addoweesh, K.E. Comparative analysis of maximum power point tracking techniques for PV applications. In Proceedings of the 16th International Multi Topic Conference, Lahore, Pakistan, 19–20 December 2013; pp. 83–88.

Mayo, J; Maldonado, Rapisarda, P; Rocha, P Stability of switched linear differential systems, IEEE Transactions on Automatic Control 59 (2014) 2038–2051.

Mahdavi. J, Emadi. A and Toliyat. H, "Application of state space averaging method to sliding mode control of PWM DC/DC converters," IAS '97. Conference Record of the 1997 IEEE Industry Applications Conference Thirty-Second IAS Annual Meeting, 1997, pp. 820-827 vol.2, DOI: 10.1109/IAS.1997.628957.

Nguyen, B., Nguyen, V., Duong, M., Le, K., Nguyen, H. and Doan, A., 2020. Propose a MPPT Algorithm Based on Thevenin Equivalent Circuit for Improving Photovoltaic System Operation. Frontiers in Energy Research, 8.

Nelson, C., 2011. 5 - LT1070 design manual. In: B. Dobkin and J. Williams, ed., Analog Circuit Design. Newnes, pp.59-123.

Pandiarajan N., Ranganath M., Mathematical Modeling of Photovoltaic Module with Simulink, 1st International Conference on Electrical Energy Systems (ICEES), 2011, p. 258-263.

Rikesh S., Moumi P., Analysis of Photovoltaic Cells with Closed Loop Boost Converter, Intr. Jour, of Advances in Eng. & Technology, 2013, 6(1), p.304-315.

Solarhub.com. 2022. SolarHub - PV Module Details: 1STH-215-P - by 1Soltech. [online] Available at: <http://www.solarhub.com/product-catalog/pv-modules/5623-1STH-215-P-1Soltech> [Accessed 28 July 2022].

Sabzi, S., Asadi, M. and Moghbelli, H., 2016. Design and Analysis of Lyapunov Function based Controller for DC-DC Boost Converter. Indian Journal of Science and Technology, 9(48).

Sera, D., Teodorescu, R., Hantschel, J. and Knoll, M., 2008. Optimized Maximum Power Point Tracker for Fast-Changing Environmental Conditions. IEEE Transactions on Industrial Electronics, 55(7), pp.2629-2637.

Salman, S., AI, X. and WU, Z., 2018. Design of a P-&-O algorithm based MPPT charge controller for a stand-alone 200W PV system. Protection and Control of Modern Power Systems, 3(1).

Taha, M.Q.; Eesse, Q.H.; Salih, S.M. Mathematical modelling of different photovoltaic modules. Journal of Telecommunication. 2011, 11, 59–64

Verma, D.; Nema, S.; Agrawal, R.; Sawle, Y.; Kumar, A. A Different Approach for Maximum Power Point Tracking (MPPT) Using Impedance Matching through Non-Isolated DC-DC Converters in Solar Photovoltaic Systems. Electronics 2022, 11, 1053. https://doi.org/10.3390/electronics11071053

Student Self-reflection on performance

All students must complete the following sections for every piece of work they submit using this template. The aim of this is to help you use feedback more effectively to improve your marks and your skills as a professional engineer. This section is not formally marked, but your tutor may use it when discussing your work with you.

Describe how you have used AT LEAST ONE of the following sources of information to improve this piece of work: **1.) (PREFERRED) Feedback from previous assignment(s). This can be from the same module or from a previous module or previous year of study (e.g. comments from 1st year lab formal reports should be used to help improve your 2nd year lab formal reports).** **2.) The marking criteria or rubric provided for this assignment.** **3.) The Department Technical Writing Handbook for Students.**
1). The previous feedback taught me how to use critical thinking to analyse and solve problems. In addition, I have improved my experiences and working independently. 2). From the marking criteria, I have learnt how to arrange my writing to get as maximum marks as possible, such as the style of the report, list of figures and tables, and etc. 3). Technical Writing Handbook was very useful for me to improve my academic writing by choosing the correct tense for each section and How to write in the third person and avoiding (I, We, and etc).
Are there any aspects of this work that you would specifically like the marker to comment/or advise on? For example: "I wasn't sure if my figure formatting looked professional and would appreciate feedback on this aspect"